Noname manuscript No.
(will be inserted by the editor)

Monotonic sampling of a continuous closed curve with respect to its Gauss digitization. Application to length estimation

É. Le Quentrec · L. Mazo · É. Baudrier · M. Tajine

the date of receipt and acceptance should be inserted later

Abstract In many applications of geometric processing, the border of a continuous shape and of its digitization (i.e. its pixelated representation) should be matched. Assuming that the continuous-shape boundary is *locally turn bounded*, we prove that there exists a mapping between the boundary of the digitization and the one of the continuous shape such that these boundaries are traveled together in a cyclic order manner. Then, we use this mapping to prove the multigrid convergence of perimeter estimators that are based on polygons inscribed in the digitization. Furthermore, convergence speed is given for this class of estimators. If, moreover, the continuous curves also have a Lipschitz turn, an explicit error bound is calculated.

Keywords digitization · integral curvature · turn · Jordan curve · perimeter discrete estimation,

1 Introduction

The estimation of a geometric feature of an object from its picture is required in several fields. One of the issues in this process is the discretization due to the image acquisition that reduces the information necessary to the estimation. Therefore, dedicated estimators are mandatory and their properties should be proved or evaluated. That is the problematic of geometric estimation in discrete geometry. Characteristics whose dimension is that of the ambient-space like area in the plane, have estimators which have been proved to be accurate (see for instance Theorem 2.2, section 2.4.2 [9] or Theorem 8 [10]). For characteristics with dimensions lower than that of the ambient space, like perimeter or curvature in the plane, the accuracy of the proposed estimators is proved on specific curves [21], [31], [10], [7], [5], or illustrated on examples [30], [20], [6], [11] [4,32]. The aim of this paper is to prove the accuracy of perimeter estimation (in a sense to be defined) for a wide class of estimators under some hypotheses on the shapes.

In the sequel of the article, we focus on the estimation of perimeter for shapes homeomorphic to a disk or equivalently to length estimation of Jordan curves.

ICube-UMR 7357, 300 Bd Sébastien Brant - CS 10413 - 67412 Illkirch Cedex FRANCE
E-mail: elequentrec@unistra.fr

We provide here a brief overview of the perimeter estimation in discrete geometry. Length estimation methods can be based on a tangent estimation [4, 14], or consist in splitting the digital boundary into *patterns* (small sequences of boundary pixels) and summing the lengths associated to each pattern. In the latter class, the choice of the pattern size determines a classification on perimeter estimation methods. One can distinguish three classes: the local estimators for which the pattern size is constant, that is, it does not depend on the curve nor on the grid step; the Semi-Local and Non-Local estimators for which the pattern size depends only on the grid step, but not on the curve; and the adaptive ones for which the number of pixels in each pattern is determined by the estimation algorithm from the discrete curve. There are two types of adaptive length estimators, the Maximal Digital Straight Segments (MDSS) and the Minimal Length Polygons (MLP).

The evaluation of the accuracy of the perimeter estimators is made through their application on curve examples [12, 4], on curve classes [14] or by verifying an asymptotic property so-called the *multigrid convergence*: the estimation error has to tend towards 0 when the grid step tends to 0. Let's take a look to this property on the three estimator classes described above. Even if the local estimators are the easiest to use, they do not verify the multigrid convergence property for an important amount of curves [29]. On one hand, adaptive estimators have been proved to be multigrid convergent on convex curves [10]. On the other hand the proofs are difficult to generalize because of the adaptability of the algorithms to each curve. Nevertheless, for adaptive estimators on curves of class C^3 with positive curvature, it has been proved in [32] that the asymptotic pattern pixel number tends to infinity and its real size tends to 0. Keeping this behaviour in their definition (without being adaptive), the Semi-Local estimators, respectively the Non-Local estimators have been proved to be multigrid convergent for functions of class C^2 [20], respectively Lipschitz functions [21]. But these results have been obtained on graphs of functions, not on curves. As the Non-Local estimators is an attempt to be a unified framework for adaptive and semi-local estimators [21], it seems relevant to extend it to planar curves. Nevertheless, the results depend on the estimators but also on the classes of the estimated curves. These classes are detailed in the next paragraph.

The length estimation error is always given for an estimator class on a class of curves (Table 1). In order to perform a geometric estimation on a curve, and taking into account the small quantity of information contained in its digitization, the complexity of the curve should be upper bounded. Geometric hypotheses on the continuous curve are needed to control this quantity of information. These geometric hypotheses should be invariant by rigid transformation and determine the grid step for which the digitization will encompass enough information to perform geometric estimation. One of the most used hypothesis in discrete geometry is the par(r)-regularity. It was introduced by Pavlidis in [25], its definition was rephrased by Serra in [26], and by Latecki et al. in [16]. Par(r)-regular curves verify some regularity hypotheses. In particular, polygons are not par-regular. There exist several attempts to generalize par(r)-regularity in order to include shapes with spikes: half-regularity [28], r-stability [22], quasi(r)-regularity [24], the μ-reach [3]. But none of them excludes artifacts of the continuous curve that prevent accurate length estimation. In addition to these original papers, the reader can

Estimator	Class of curves	Proof of multigrid convergence	Rate of convergence
MDSS	convex C^3 with positive curvature	Thm 5.36 [14]	O($h^{1/3}$)
	convex polygons	Thm 12 [10]	$O(h)$
GC-MLP	convex curves	for Jordan digitization scheme Thm 4.15 [27]	O(h)
AS-MLP	convex polygon	Thm 2 [2]	$O(h)$
Non-local estimator	graph of Lipschitz function	Cor 1 [21]	-
	graph of $C^{1,1}$ function	Cor 2 [21]	$O(M_1^h + \frac{h}{M_1^h})$
MDSS	graph of Lipschitz function	Thm 8 [21]	-

Table 1: The table gives the proved worst-case rate of convergence of several estimators on a specific class of curves. When not specified the convergence is studied for the Gauss digitization scheme. The class $C^{1,1}$ gathers functions whose derivative are Lipschitz.

find a little more detailed presentation of the above notions in our previous paper about locally turn bounded curves [18]. [1].

In this article, we aim at providing a proof of multigrid convergence for some perimeter estimators and to bound their worst-case error on a wide class of Jordan curves including both regular curves and polygons. In order to define such a class of curves, we choose to use a criterion based on the *turn* of the curve, which is a generalization of the integral of the curvature along the curve [1]. Indeed the turn is the amount by which a curve deviates from being a straight line. In this article, we consider two families of curves: the curves having a turn being a Lipschitz function of their length and the curves whose small arcs have a bounded turn (*locally turn-bounded* curves, see Definition 1). The notion of local turn-bounded curve (LTB-curve) was introduced in a previous work [18].

Let us introduce the digitization process used in this article. Given a shape S and a grid step h, the Gauss digitization of S denoted by $\mathrm{Dig}_h(S)$, is the discrete subset of $S \cap h\mathbb{Z}^2$. The *reconstruction* of S is the Minkowski sum $\mathrm{Dig}_h(S) \oplus P$ where $P = [-h/2, h/2]^2$. A boundary element of a digitized shape S, usually called a *bel* is composed of a pair of 4-adjacent grid points, one lying outside the shape and the other lying inside the shape, or on its boundary see Figure 1.

Since bounding the error of a non-local estimator consists in comparing the length of the curve and the length of a polygon whose vertices are derived from the digitization, an important step is to associate the edges of the polygon to arcs partitioning the continuous curve. In other words, we want to define a mapping from the ordered set of the digitization bels to an ordered sequence of points on the continuous curve $\mathcal{C}$. Furthermore, in order to guarantee the multigrid convergence, each bel has to be close to its image. In [13], the whole continuous curve is associated point by point to the boundary of its reconstruction using the projection

[1] Other hypotheses can be chosen for curves that are graphs of a function: the function or its derivatives can be required to be Lipschitz (see [21])

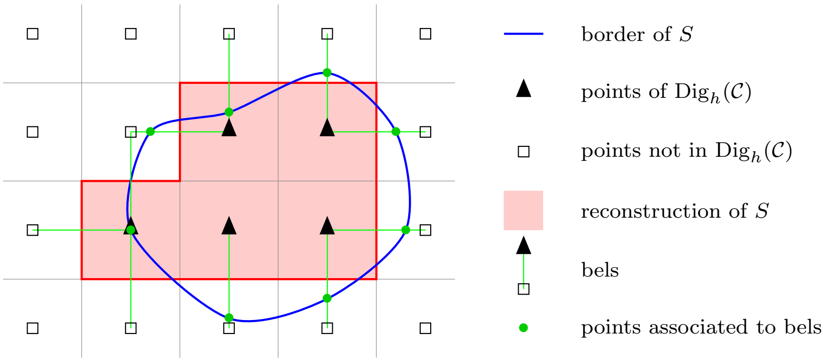

Figure 1: Each bel is associated to an intersection point of itself and the border of the shape S. In the general case, there is no guarantee that the cyclic order on bels implies a cyclic order on the border of the shape. In Section 3, we will prove that locally turn bounded curves makes it possible to define such a monotonic association.

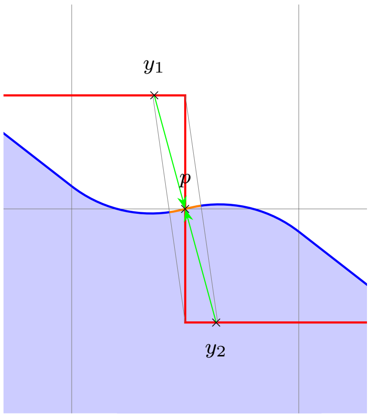

Figure 2: ([14, Figure B.2]) In blue and orange a Jordan curve $\mathcal{C}$, in red the boundary $\partial_h(\mathcal{C})$ of the reconstruction of its interior. The projection on the curve $\mathcal{C}$ restricted to $\partial_h(\mathcal{C})$ is represented by the green arrows. The points y_1 and y_2 have the same image p by the projection on the curve. The set of points of $\partial_h(\mathcal{C})$ having at least two preimages by the projection is represented in orange. When a point y in $\partial_h(\mathcal{C})$ moves from left to right, this orange part is traveled three times.

to nearest point defined in [8]. This projection is well-defined only for sets having a positive reach, that is, for par-regular curves. Moreover, this projection is onto but not order-preserving (see Figure 2) even if the length of the "non-injective" part of the projection on $\mathcal{C}$ can be upper bounded [13]. Notice that this step is not always necessary: for small classes of curves as the convex polygons, the bounding of estimation error is based on other arguments (see [10]).

Our contribution is twofold. The first and main contribution of the article is to define a mapping (Definition 6) from bels to points on the curve and to prove that this mapping is order-preserving. Besides, we show that the mapping partitions the curve in arcs of limited turns. The whole section 3 is dedicated to this proof. The second contribution is the length estimation for locally turn-bounded curves. We prove the multigrid convergence of some Non-Local estimators (Theorem 2 and Theorem 3). We also provide rates of convergence depending on the mean and maximal size of patterns. Moreover we give an explicit upper bound of the error of estimation for LTB curves with Lipschitz turn in order to enable a practical use at a fixed resolution.

2 Background: Hypotheses on the continuous shape and some consequences

In this section, we recall the definition and the main properties of *locally turn-bounded curves*. All this material comes from our previous article [18].

2.1 Turn

In this section, we recall the definition of the turn and some of its properties. The main reference is the book of Alexandrov and Reshetnyak [1]. Nevertheless, the reader will find in our previous article [18] two pages presenting these properties with some comments and precise references inside the book.

Generally, the convergence of geometrical estimators is given under analytical hypothesis on the continuous curve. In most of the cases, the continuous curve is supposed to be twice differentiable. But as noticed in [1]:

"It should be remarked that differential geometry commonly studies only the curves obeying certain conditions of regularity. These conditions are imposed by the requirement that the apparatus of differential calculus be applied, but they are hardly justified in a geometrical sense." In this article, we choose to study geometrical features of the continuous curve based on the turn. In order to be able to consider both polygons and regular curves, we use the definition of the turn given in [1], [23]. But beforehand, let us clarify some notations.

- For practical reasons, a sequence of points (a_i) of a closed curve is indexed by the quotient group $\mathbb{Z}/N\mathbb{Z}$. This allows for instance to use the equality $a_N = a_0$. In particular, this notation will be used for the vertices of a polygon. The subset $\{i, i+1, ..., j\}$ of $\mathbb{Z}/N\mathbb{Z}$ is denoted by $[\![i, j]\!]$ and $\#[\![i, j]\!]$ stands for the cardinal of $[\![i, j]\!]$.
- The angle between two vectors $\vec{u}$ and $\vec{v}$ is denoted by $(\vec{u}, \vec{v})$ ($(\vec{u}, \vec{v}) \in \mathbb{R}/2\pi\mathbb{Z}$). The geometric angle between two vectors $\vec{u}$ and $\vec{v}$, or between two directed straight lines oriented by $\vec{u}$ and $\vec{v}$, is denoted by $\angle(\vec{u}, \vec{v})$. It is the absolute value of the reference angle taken in $(-\pi, \pi]$ between the two vectors. Thus, $\angle(\vec{u}, \vec{v}) \in [0, \pi]$. Given three points x, y, z, we also write $\widehat{xyz}$ for the geometric angle between the vectors $x - y$ and $z - y$.

We now give the definition of the turn.

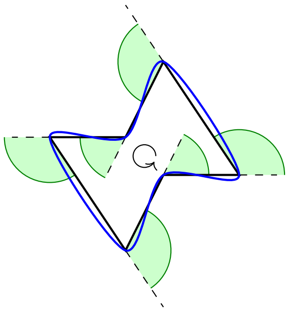

Figure 3: The turn of the inscribed polygon is the sum of green angles. The turn of the blue Jordan curve it the supremum of turn of inscribed polygons

- *The turn* $\kappa(L)$ of a polygonal line $L = [x_i]_{i=0}^{N-1}$ is defined by:

$$\kappa(L) := \sum_{i=1}^{N-2} \angle(x_i - x_{i-1}, x_{i+1} - x_i) \ .$$

- *The turn* $\kappa(P)$ of a polygon $P = [x_i]_{i\in\mathbb{Z}/N\mathbb{Z}}$ is defined by (see Figure 3):

$$\kappa(P) := \sum_{i\in\mathbb{Z}/N\mathbb{Z}} \angle(x_i - x_{i-1}, x_{i+1} - x_i) \ .$$

- In the rest of the paper, we write $C_{a,b}$ for an arc of curve between the points a and b; moreover, the topology on the curve and its arcs is the topology induced on the curve, therefore, an open arc $\mathring{C}$ is the arc C minus its endpoints.
- A sequence (a_j) of points of a simple closed curve $\mathcal{C}$ forms a *chain* if for each pair (i, j), the intersections of the two open arcs of $\mathcal{C}$ from a_i to a_j with the set $\{a_k\}$ are exactly the subsets $\{a_k\}_{k\in[\![i+1,j-1]\!]}$ and $\{a_k\}_{k\in[\![j+1,i-1]\!]}$.
- A polygonal line (or a polygon) is said to be *inscribed* in $\mathcal{C}$ if its ordered sequence of vertices forms a chain of $\mathcal{C}$.
- *The turn* $\kappa(\mathcal{C})$ of a simple curve $\mathcal{C}$ (respectively of a Jordan curve) is the supremum of the turn of its inscribed polygonal lines (respectively of its inscribed polygons).

The turn has the following properties[2]

Property 1 ([1])

- The turn coincides with the integral of the usual curvature on C^2 curves.
- (Fenchel's Theorem) The turn of a Jordan curve is greater than or equal to 2π. The equality case occurs if and only if the interior of $\mathcal{C}$ is convex.
- Every curve of finite turn has left-hand and right-hand tangent vectors $e_l(c)$ and $e_r(c)$ at each of its points.
- For any arc $C_{a,b}$ of finite turn containing a point c,

$$\kappa(C_{a,b}) = \kappa(C_{a,c}) + \kappa(C_{c,b}) + \angle(e_l(c), e_r(c)).$$

[2] About these properties, the reader can find in [18] some comments and more precise references.

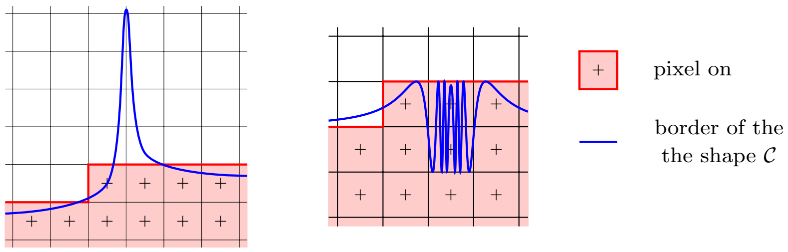

Figure 4: The curve on the left has a thin spike avoiding all the centers of pixels. Alike, we can build curves having arcs arbitrarily far from their Gauss digitization. Even if the curve stay close to its digitization, it can oscillate a lot around its digitization. Such artifacts can induce for instance an arbitrarily big difference between the length of the curve and the length of its digitization.

– For any Jordan curve $\mathcal{C}$ of finite turn containing a point c,

$$\kappa(\mathcal{C}) = \kappa(\mathcal{C} \setminus \{c\}) + \angle(e_l(c), e_r(c)).$$

2.2 Local turn-boundedness

We introduced in [17] a new local geometric feature based on the turn. It consists in locally bounding the turn of the curve in order to forbid the artifacts depicted in Figure 4. This new feature allows us to consider a wider class than the par-regular curves usually used for estimation in discrete geometry.

Definition 1 (LTB curves [17]) A Jordan curve $\mathcal{C}$ is (θ, δ)-*locally turn-bounded* ((θ, δ)-LTB) if, for any two points a and b in $\mathcal{C}$ such that the Euclidean distance $\mathrm{d}(a, b) < \delta$, the turn of one of the arcs of the curve $\mathcal{C}$ delimited by a and b is less than or equal to θ.

In particular it forbids the *angular points* in $\mathcal{C}$ of turn greater than θ, i.e. points c for which $\angle(e_l(c), e_r(c)) > \theta$ (see [17, Proposition 3]).

Hereafter, we recall the properties of the LTB-curves that will be used in this paper.

The first property links the parameter δ of a LTB curve with the diameter of the curve.

Property 2 ([18], Lemma 1) The diameter of a closed $(2\pi/3, \delta)$-LTB curve is at least δ.

Notice that two distinct points of a Jordan curve delimit two arcs of the curve. To distinguish these two arcs, we introduced in [17] the notion of *straightest arc*.

Property 3 ([18, Lemma 2]) Let $\mathcal{C}$ be a $(\pi/2, \delta)$-LTB curve. Let a, b be points of $\mathcal{C}$ such that $\mathrm{d}(a, b) < \delta$. Then there exists a unique arc of $\mathcal{C}$ delimited by the points a and b and whose turn is less than or equal to $\frac{\pi}{2}$.

Definition 2 (Straightest arc, [18, Definition 6]) Let $\mathcal{C}$ be a $(\pi/2, \delta)$-LTB curve. Let a, b be points of $\mathcal{C}$ such that $\mathrm{d}(a, b) < \delta$. The unique arc of $\mathcal{C}$ delimited by the points a and b and whose turn is less than or equal to $\frac{\pi}{2}$ is called *the straightest arc between a and b* and noted $\boldsymbol{C}_{a,b}$.

Since the notion of straightest arc is a key tool in this article, we set $\theta = \pi/2$ for the rest of the paper and we write δ-LTB instead of $(\pi/2, \delta)$-LTB.

Property 4 ([18, Proposition 4]) Let $\mathcal{C}$ be a δ-LTB curve. Let a, b be two points of $\mathcal{C}$ such that $\mathrm{d}(a, b) < \delta$. The straightest arc $\boldsymbol{C}_{a,b}$ between a and b is included in the disk of diameter $[a, b]$.

Local turn-boundedness can be understood as a constraint on the thickness of the interior of the curve $\mathcal{C}$. Indeed, the intersection of $\mathcal{C}$ with any open disk centered in a point of $\mathcal{C}$ and of radius less than or equal to δ is path-connected.

Property 5 ([18], Proposition 5) Let $\mathcal{C}$ be a δ-LTB Jordan curve and $a \in \mathcal{C}$. Then, for any $\epsilon \leq \delta$, the intersection of $\mathcal{C}$ with the open disk $B(a, \epsilon)$ is path-connected and is therefore an arc of $\mathcal{C}$.

From Property 5, we derive that, in each ball of radius $\delta/2$ centered on a LTB curve point a, the Euclidean distance to a increases along the curve.

Property 6 ([18, Proposition 12]) Let $\mathcal{C}$ be a δ-LTB curve. Let $\gamma\colon [0, t_M) \to \mathcal{C}$ be an injective parametrization of the curve $\mathcal{C}$ and $t_m \in (0, t_M)$ be such that the arc $\gamma([0, t_m])$ is included in $B(\gamma(0), \frac{\delta}{2})$. Then, the restriction of the function $t \mapsto \|\gamma(t) - \gamma(0)\|$ to $[0, t_m]$ is increasing.

The preservation by the digitization process of topological properties as connectedness, or manifoldness, requires to discretize continuous objects with sufficiently tight grids. In the framework of LTB curves, this is expressed by the notion of grid, and also of square, *compatible with* a (LTB) curve presented here (Definition 3).

Definition 3 ([18], Definition 9) Let $\mathcal{C}$ be a δ-LTB curve. A grid with step h, or a square of side length h, is said to be *compatible* (with the curve $\mathcal{C}$) if h is strictly smaller than $\min(\frac{\sqrt{2}}{2}\delta, \frac{1}{2}\operatorname{diam}(\mathcal{C}))$.

Any δ-LTB curve yields 4-connected and well-composed discretizations [15] on compatible grids.

Property 7 ([18], Proposition 9) Let $\mathcal{C}$ be a δ-LTB curve. Then, the Gauss digitization of $\mathcal{C}$ on any compatible grid is 4-connected and well-composed.

The value of $\theta \leq \frac{\pi}{2}$ and $\sqrt{2}h < \delta$ are tight. Two counterexamples are shown in Figure 5.

The constraint on the curvature of a LTB curve makes it possible to describe with accuracy the behavior of such a curve with respect to compatible grid pixels. This was expressed in [18] through the notion of "arc passing through" a pixel.

Definition 4 ([18], Definition 8 and Proposition 7) Given a LTB curve $\mathcal{C}$ and a compatible square T, there exists a maximal (for the inclusion) straightest arc of $\mathcal{C}$ with endpoints in T. It is called the *T-straightest arc* of $\mathcal{C}$ and it its denoted by $\boldsymbol{C}_T$ (see Figure 6) .

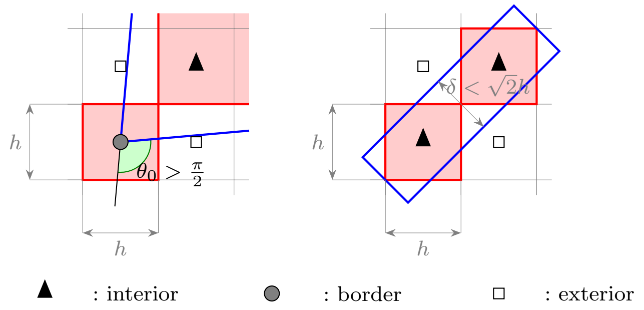

Figure 5: [18, Figures 14,15] Two examples of curve not compatible with the grid and having a not well-composed Gauss digitization, that is a Gauss digitization with a "cross configuration". A cross configuration is a square of side-length h having two diagonally opposed vertices in the Gauss digitization and the two others not belonging to the Gauss digitization. The black triangles designate integer points belonging to the Gauss digitization of the blue shape, the gray circle designates an integer point belonging to the border of the blue shape (hence belonging to the Gauss digitization) and the white squares designate two integer points outside the Gauss digitization.

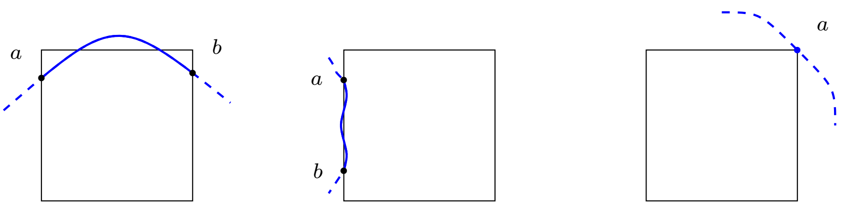

Figure 6: On each of the three blue curves, the square-straightest arc is depicted by a continuous line whereas the rest of the curve is dashed. On the left and on the middle the square-straightest arc is delimited by the points a and b, on the right, the square-straightest arc is reduced to the point a.

Be aware that we have changed the designation of the arc passing through T from [18] into T-straightest arc .

The T-straightest arc has the following localization property.

Property 8 ([18], Proposition 6) Let $\mathcal{C}$ be a δ-LTB curve and T be a compatible square. Then, the T-straightest arc of $\mathcal{C}$ is included in the *swelling of* T which is the union of the four disks whose diameters are the sides of T (see Figure 7). Furthermore, the complement of $\boldsymbol{C}_T$ in $\mathcal{C}$, the open arc $\mathcal{C} \setminus \boldsymbol{C}_T$, does not intersect T.

Thanks to the notion of T-straightest arc, we are able to locally distinguish exterior points from interior points. The notion of swelling of T corresponds to the swollen set of T defined in [18],we change the designation in this article.

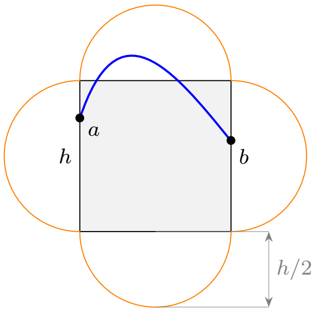

Figure 7: The straightest arc of the square is included in the swelling of the square.

Property 9 ([18], Proposition 8) Let $\mathcal{C}$ be a δ-LTB Jordan curve and T be a compatible square. Let a, b be the endpoints of the T-straightest arc of $\mathcal{C}$. Two vertices of the square T are in the same connected component of $\mathbb{R}^2 \setminus \mathcal{C}$ if and only if they are in the same connected component of $T \setminus [a, b]$ and they do not lie on $\mathcal{C}$.

The following property considers the case when the T-straightest arc contains a vertex of the square T.

Property 10 ([18], Lemma 4) Let $\mathcal{C}$ be a δ-LTB Jordan curve and T be a compatible square. Suppose that the square T has a vertex v lying on $\mathcal{C}$. Then, either this vertex v is an endpoint of the T-straightest arc of $\mathcal{C}$, or the T-straightest arc is wholly included in the two sides of T having v for endpoint.

We end this section about local turn boundedness by a new result that is just a set of technical improvements of some of the properties mentioned above. These new statements are used in Section 3.

Lemma 1 *Let $C_{a,b}$ be a subarc of a δ-LTB Jordan curve such that $\mathrm{d}(a, b) < \delta$.*

(a) The arc $C_{a,b}$ is the straightest arc between a and b if and only if it is included in the disk whose diameter is the straight segment $[a, b]$.
(b) If the arc $C_{a,b}$ is the straightest arc between a and b, then,

$$< e_l(a), e_r(a) > +\kappa(C_{a,b})+ < e_l(b), e_r(b) > \leq \frac{\pi}{2}.$$

Proof

(a) The "only if" part of the assertion is stated in Property 4. The "if" part results from Property 2. Indeed, if $C_{a,b}$ is included in the disk D whose diameter is $[a, b]$ where $\mathrm{d}(a, b) < \delta$, by Property 2, the other arc between a and b, say $C_{b,a}$, is not included in D. Thus, from the "only if" part, $C_{b,a}$ is not the straightest arc from a to b. As, according to Definition 2, the straightest arc exists, it is $C_{a,b}$.
(b) The idea is to slightly extend the arc $\boldsymbol{C}_{a,b}$ on both sides so as to include the points a and b in its interior while keeping the distance between the extremities under the threshold value δ. Nevertheless, we have to justify that the extended arc is still a straightest arc.

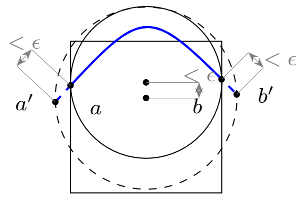

Figure 8: The proof of Lemma 1 b) consist on extending the straightest arc between a and b into an arc $\mathcal{C}_{a',b'}$ between a' and b' and then in showing that $\mathcal{C} \setminus \mathcal{C}_{a',b'}$ is not included in the disk of diameter $[a', b']$.

So, let a' and b' be the extremities of the extended arc $C_{a',b'}$: $a' \notin \boldsymbol{C}_{a,b}$, $b' \notin \boldsymbol{C}_{a,b}$, $C_{a',b'} = \boldsymbol{C}_{a',a} \cup \boldsymbol{C}_{a,b} \cup \boldsymbol{C}_{b,b'}$. Let $\varepsilon = (\delta - \mathrm{d}(a,b))/4$. We choose a' and b' such that $\mathrm{d}(a,a') < \varepsilon$ and $\mathrm{d}(b,b') < \varepsilon$ (see Figure 8). Then, $\mathrm{d}(a',b') < \delta - 2\varepsilon$. Furthermore, it can be proved that the distance between the center of the open disk D whose diameter is $[a,b]$ and the open disk D' whose diameter is $[a',b']$ is less than ε. Thanks to the triangle inequality, we derive that D' is included in the open disk D_+ whose center is the midpoint of $[a,b]$ and whose diameter is δ. Furthermore, the straightest arcs $\boldsymbol{C}_{a',a}$ and $\boldsymbol{C}_{b,b'}$ are included in D_+ by the choice of ε and Property 4. Then, $\boldsymbol{C}_{a',a} \cup \boldsymbol{C}_{a,b} \cup \boldsymbol{C}_{b,b'} \subset D_+$, $D' \subset D_+$ but the whole curve $\mathcal{C}$ is not included in D_+ (by Property 2). It comes that $\mathcal{C} \setminus \left(\boldsymbol{C}_{a',a} \cup \boldsymbol{C}_{a,b} \cup \boldsymbol{C}_{b,b'}\right)$ is not included in D' and for this reason cannot be the straightest arc from a' to b'. Hence $\boldsymbol{C}_{a',a} \cup \boldsymbol{C}_{a,b} \cup \boldsymbol{C}_{b,b'}$ is the straightest arc between a' and b'. $\square$

3 Digitization based partition of a LTB curve

One main objective of this article is to map the boundary of a discretized object onto the continuous original object thanks to small displacements of the discrete boundary while keeping the order on the boundary of the discrete object. This is the purpose of this section.

Note that the proofs given in Section 3 rely on the properties of LTB curves recalled in Section 2.2.

3.1 Back-digitization

We begin by some vocabulary and notations that will be used throughout Section 3.

Let $p \in \mathbb{R}^2$ and $h \in (0, +\infty)$. We denote by P_p the square $p \oplus P$ where $P = [-h/2, h/2]$. When $p \in h\mathbb{Z}^2$, we say that P_p is a *pixel* and when $p \in (h/2, h/2) + h\mathbb{Z}^2$, we say that P_p is a *dual pixel*. Observe that the vertices of a dual pixel all have integer coordinates.

Given a Jordan curve $\mathcal{C}$ surrounding a shape S and given a grid step h, we recall that a *bel* (for "boundary element") is an ordered pair of 4-adjacent grid points, the first point lying inside the shape, or on its boundary and the second point lying outside the shape. By abuse of language, a bel is identified with the segment linking its two points. The set of all the bels obtained from $\mathrm{Dig}_h(S)$ is denoted $\mathrm{Bel}_h(\mathcal{C})$.

A dual pixel containing a bel is called a *boundary dual pixel*, or BDP for short. Obviously, a bel always belongs to two BDPs. Conversely, it is plain that in a well-composed digitization, a BDP contains exactly two bels (see Figure 9). That way, the graph whose vertex set is $\mathrm{Bel}_h(\mathcal{C})$ and whose edges are the pairs of bels belonging to a same dual pixel is regular with degree 2. If the graph $\mathrm{Bel}_h(\mathcal{C})$ is connected, $\mathrm{Bel}_h(\mathcal{C})$ may be equipped with a cyclic order and when we need to consider this cyclic order, we put $\mathrm{Bel}_h(\mathcal{C}) = (b_i)_{i\in\mathbb{Z}/N\mathbb{Z}}$. We derive from Property 7 that if the grid is compatible with $\mathcal{C}$, $\mathrm{Bel}_h(\mathcal{C})$ is equipped with a cyclic order.

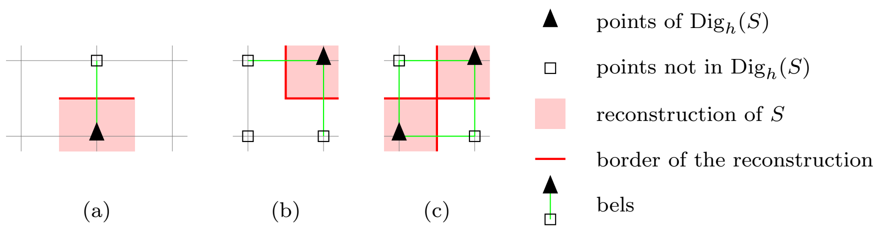

Figure 9: Let S be a shape homeomorphic to a closed disk. Its boundary is a Jordan curve, we call it $\mathcal{C}$. (a) Each edge of the boundary of the reconstruction of the shape S separates a grid point outside S and one adjacent grid point in S. Then the bels of $\mathrm{Dig}_h(S)$ and the edges of the reconstruction are in one-to-one correspondence. (b) and (c): When the digitization of S is well-composed, no BDP contains the cross configuration (c). Then each BDP contains exactly two bels (b).

From Jordan's Curve Theorem, we derive that each segment in $\mathrm{Bel}_h(\mathcal{C})$ intersects the curve $\mathcal{C}$. The notion of *back-digitization* defined hereafter corresponds to a mapping from bels to such intersection points. Since we want our mapping to preserve the bel order but we cannot impose injectivity (see Figure 10), we have to relax the notion of chain (see Section 2.1) to sequences of curve points having several consecutive occurrences of the same point.

Definition 5 (semi-chain) Let $N \geq 1$. A sequence $(\xi_k)_{k\in\mathbb{Z}/N\mathbb{Z}}$ of points of a simple closed curve $\mathcal{C}$ forms a *semi-chain* if for each pair (i, j), the intersections of the two closed arcs of $\mathcal{C}$ between ξ_i and ξ_j with the set $\{\xi_k\}_{k\in\mathbb{Z}/N\mathbb{Z}}$ are the subsets $\{\xi_k\}_{k\in[\![i,j]\!]}$ and $\{\xi_k\}_{k\in[\![j,i]\!]}$ (see Figure 11 a). Given a δ-LTB curve $\mathcal{C}$, a semi-chain $(\xi_k)_{k\in\mathbb{Z}/N\mathbb{Z}}$ of $\mathcal{C}$ is a *sampling semi-chain* if, for any $k \in \mathbb{Z}/N\mathbb{Z}$, $\mathrm{d}(\xi_k, \xi_{k+1}) < \delta$ and the open straightest arc of $\mathcal{C}$ between ξ_k and ξ_{k+1} does not intersect $\{\xi_k\}_{k\in\mathbb{Z}/N\mathbb{Z}}$.

An example of a semi-chain not being a sampling semi-chain is given in Figure 11 b. Observe that any Jordan curve point sequence whose cardinal is less than 4 is a semi-chain.

The two following lemmas give some properties of (sampling) semi-chains.

Lemma 2 *Let $\mathcal{C}$ be δ-LTB curve and $(\xi_k)_{k\in\mathbb{Z}/N\mathbb{Z}}$ be a semi-chain of $\mathcal{C}$. If $\xi_i = \xi_j$ for some $i, j \in \mathbb{Z}/N\mathbb{Z}$ then $\{\xi_k\}_{k\in[\![i,j]\!]}$ or $\{\xi_k\}_{k\in[\![j,i]\!]}$ is a singleton.*

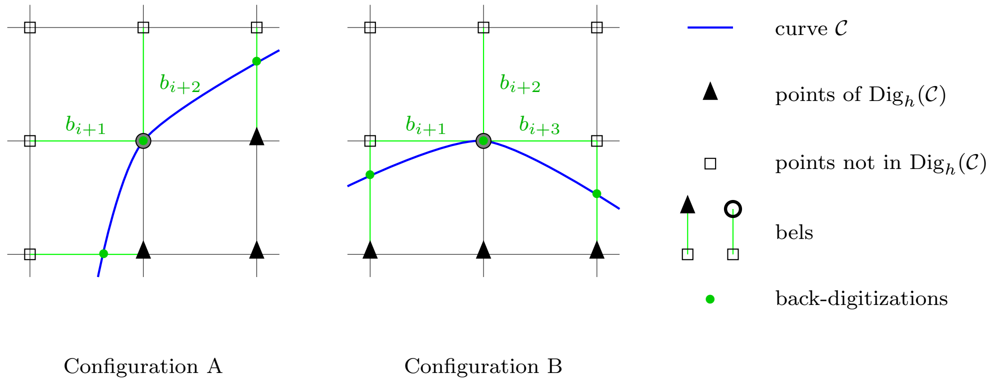

Figure 10: Consecutive bels (left: 2 bels, right: 3 bels) have to be back-digitized on the same point of the curve.

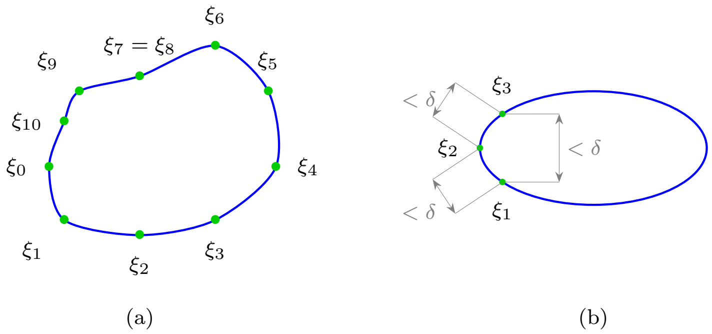

Figure 11: a) The sequence $(\xi_k)_{k=0}^{10}$ is a semi-chain of the blue Jordan curve. For instance, the intersections of the set $\{\xi_k\}_{k\in\mathbb{Z}/11\mathbb{Z}}$ with the two arcs of the blue curve between ξ_3 and ξ_8 are the subsets $\{\xi_8, \xi_9, \xi_{10}, \xi_0, \xi_1, \xi_2, \xi_3\}$ and $\{\xi_3, \xi_4, \xi_5, \xi_6, \xi_7, \xi_8\}$ (since $\xi_7 = \xi_8$). b) The sequence $(\xi_k)_{k=1}^{3}$ is a semi-chain that is not a sampling semi-chain. Any two points in $\{\xi_1, \xi_2, \xi_3\}$ are at distance strictly less than δ, but the open straightest arc between ξ_1 and ξ_3 contains ξ_2.

Proof This is a direct consequence of the definition of a semi-chain applied to the arcs between ξ_i and ξ_j.

Lemma 3 explains the designation “sampling” semi-chain. Indeed, given a sampling semi-chain $(\xi_i)_{i\in\mathbb{Z}/N\mathbb{Z}}$, each point p of the curve $\mathcal{C}$ is on a straightest arc between two consecutive points of this semi-chain. Thereby, and because the straightest arc between two points a and b is included in the disk whose diameter is $[a, b]$ (Property 4), each point p of the curve $\mathcal{C}$ is at distance less than δ of a point of $(\xi_i)_{i\in\mathbb{Z}/N\mathbb{Z}}$. In the following lemma, the standard notation $A \sqcup B$ denotes the disjoint union.

Lemma 3 *Let $\mathcal{C}$ be a δ-LTB curve and $(\xi_k)_{k\in\mathbb{Z}/N\mathbb{Z}}$ be a sampling semi-chain of $\mathcal{C}$ such that the cardinal of the set $\{\xi_k\}$ is greater than 2. Then,*

$$\mathcal{C} = \{\xi_k\}_{k\in\mathbb{Z}/N\mathbb{Z}} \sqcup \bigsqcup_{k\in\mathbb{Z}/N\mathbb{Z}} \mathring{\boldsymbol{C}}_{\xi_k,\xi_{k+1}} \ .$$

In particular, for any $(i,j)\in\mathbb{Z}/N\mathbb{Z}$, the arcs of $\mathcal{C}$ from ξ_i to ξ_j are

$$\{\xi_k\}_{k\in[\![i,j]\!]} \sqcup \bigsqcup_{k\in[\![i,j]\!]} \mathring{\boldsymbol{C}}_{\xi_k,\xi_{k+1}} \quad \textit{and} \quad \{\xi_k\}_{k\in[\![j,i]\!]} \sqcup \bigsqcup_{k\in[\![j,i]\!]} \mathring{\boldsymbol{C}}_{\xi_k,\xi_{k+1}} \ .$$

Proof Firstly, observe that, thanks to the assumption $\mathrm{d}(\xi_k,\xi_{k+1}) < \delta$, the arc $\mathring{\boldsymbol{C}}_{\xi_k,\xi_{k+1}}$ is well-defined.

- First, let us prove that the sets $\mathring{\boldsymbol{C}}_{\xi_i,\xi_{i+1}}$, $\mathring{\boldsymbol{C}}_{\xi_{i'},\xi_{i'+1}}$ and $\{\xi_k\}_{k\in\mathbb{Z}/N\mathbb{Z}}$ are disjoint whenever $i\neq i'$. Let i and i' be two different classes in $\mathbb{Z}/N\mathbb{Z}$. Since the sequence $(\xi_k)_{k\in\mathbb{Z}/N\mathbb{Z}}$ is a sampling semi-chain of $\mathcal{C}$, the open arc $\mathring{\boldsymbol{C}}_{\xi_i,\xi_{i+1}}$ does not contain any ξ_k, $k\in\mathbb{Z}/N\mathbb{Z}$. Therefore, $\mathring{\boldsymbol{C}}_{\xi_i,\xi_{i+1}} \cap \{\xi_k\}_{k\in\mathbb{Z}/N\mathbb{Z}} = \emptyset$ and $\mathring{\boldsymbol{C}}_{\xi_i,\xi_{i+1}} \cap \mathring{\boldsymbol{C}}_{\xi_{i'},\xi_{i'+1}} = \emptyset$ if $\{\xi_i,\xi_{i+1}\} \neq \{\xi_{i'},\xi_{i'+1}\}$. Assume that $\{\xi_i,\xi_{i+1}\} = \{\xi_{i'},\xi_{i'+1}\}$. If $\xi_i = \xi_{i+1}$, then we immediately have $\mathring{\boldsymbol{C}}_{\xi_i,\xi_{i+1}} \cap \mathring{\boldsymbol{C}}_{\xi_{i'},\xi_{i'+1}} = \emptyset$. Now, by contradiction, assume that $\xi_i \neq \xi_{i+1}$ (and thus, $\xi_{i'} \neq \xi_{i'+1}$). Two cases are possible : either $\xi_i = \xi_{i'}$ and $\xi_{i+1} = \xi_{i'+1}$, or $\xi_i = \xi_{i'+1}$ and $\xi_{i+1} = \xi_{i'}$.
  - In the first case, $\mathcal{C}$ is the union of the two closed arcs between ξ_i and $\xi_{i'}$. As $\xi_i = \xi_{i'}$, the two arcs are $\{\xi_i\}$ and $\mathcal{C}$. Since $i+1\in[\![i,i']\!]$ and $i'+1\in[\![i',i]\!]$, by definition of a semi-chain, one of the two points ξ_{i+1} and $\xi_{i'+1}$ belongs to the arc between ξ_i and $\xi_{i'}$ reduced to $\{\xi_i\}$. Since $\xi_{i+1} = \xi_{i'+1}$, $\{\xi_i,\xi_{i+1}\}$ is a singleton. Contradiction !
  - In the second case ($\xi_i = \xi_{i'+1}$ and $\xi_{i+1} = \xi_{i'}$), by Lemma 2, we derive that either $\{\xi_k\}_{k\in[\![i,i'+1]\!]}$ or $\{\xi_k\}_{k\in[\![i'+1,i]\!]}$ is a singleton and either $\{\xi_k\}_{k\in[\![i',i+1]\!]}$ or $\{\xi_k\}_{k\in[\![i+1,i']\!]}$ is a singleton. There are four possibilities which can be reduced to two thanks to the symmetry swapping i and i'. If $\{\xi_k\}_{k\in[\![i,i'+1]\!]}$ and $\{\xi_k\}_{k\in[\![i',i+1]\!]}$ are singletons, we derive that $i = i'+1$ and $i+1 = i'$ (for we assumed $\xi_{i+1}\neq\xi_i$ and $\xi_{i'+1}\neq\xi_{i'}$). It comes that $i = i+2$ in $\mathbb{Z}/N\mathbb{Z}$. That is, $N = 2$: a contradiction. If $\{\xi_k\}_{k\in[\![i,i'+1]\!]}$ and $\{\xi_k\}_{k\in[\![i+1,i']\!]}$ are singletons, we derive that $i = i'+1$ and the set $\{\xi_k\}_{k\in[\![i+1,i'+1]\!]} = \{\xi_k\}_{k\in[\![i+1,i]\!]}$ is a pair. Since, $\{\xi_k\}_{k\in[\![i,i+1]\!]}$ is also a pair, we get again $N = 2$.
- The arc $\bigsqcup_{k\in\mathbb{Z}/N\mathbb{Z}} \mathring{\boldsymbol{C}}_{\xi_k,\xi_{k+1}} \sqcup \{\xi_k\}_{k\in\mathbb{Z}/N\mathbb{Z}}$, which can be written as $\{\xi_0\} \sqcup \mathring{\boldsymbol{C}}_{\xi_0,\xi_1} \sqcup \{\xi_1\} \sqcup \cdots \sqcup \mathring{\boldsymbol{C}}_{\xi_{-1},\xi_0}$, is a simple closed arc of $\mathcal{C}$ that is not reduced to a singleton for the cardinal of the semi-chain (ξ_k) is greater than 1. Then, $\bigsqcup_{k\in\mathbb{Z}/N\mathbb{Z}} \mathring{\boldsymbol{C}}_{\xi_k,\xi_{k+1}} \sqcup \{\xi_k\}_{k\in\mathbb{Z}/N\mathbb{Z}}$ is equal to $\mathcal{C}$.
- Alike, the arcs $\bigsqcup_{k\in[\![i,j]\!]} \mathring{\boldsymbol{C}}_{\xi_k,\xi_{k+1}} \sqcup \{\xi_k\}_{k\in[\![i,j]\!]}$ and $\bigsqcup_{k\in[\![j,i]\!]} \mathring{\boldsymbol{C}}_{\xi_k,\xi_{k+1}} \sqcup \{\xi_k\}_{k\in[\![j,i]\!]}$ are simple arcs of $\mathcal{C}$ between ξ_i and ξ_j and they are not equal if $\{\xi_k\}_{k\in[\![i,j]\!]} \neq \{\xi_k\}_{k\in[\![j,i]\!]}$. So, by contradiction, assume that $\{\xi_k\}_{k\in[\![i,j]\!]} = \{\xi_k\}_{k\in[\![j,i]\!]}$. Since $\#\{\xi_k\} > 2$, there exist $\ell\in[\![i,j]\!]$ and $\ell'\in[\![j,i]\!]$ such that $\xi_\ell = \xi_{\ell'}$ and $\xi_\ell \notin \{\xi_i,\xi_j\}$. Finally, applying Lemma 2 to ξ_ℓ and $\xi_{\ell'}$, we get $\xi_i = \xi_\ell$ or $\xi_j = \xi_\ell$: a contradiction. □

We can now define the main notion provided by this article.

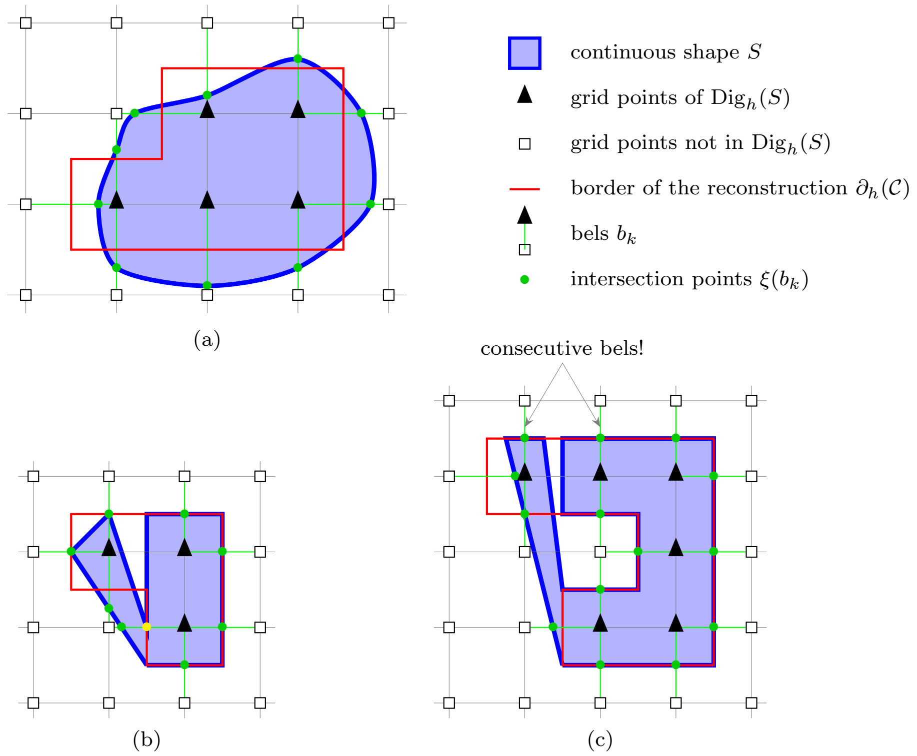

Figure 12: Two bels are consecutive if they are edges of the same BDP (Boundary Dual Pixel). The order on the bels is considered relatively to the boundary $\partial_h(\mathcal{C})$ of the reconstructed shape, but the order on the points $\xi(b_k)$ back-digitized from bels is considered relatively to the continuous Jordan curve $\mathcal{C}$. Example (a): a simple case: there is a unique mapping ξ linking bels to their green points, it is injective and the sequence of green points form a semi-chain of $\mathcal{C}$. Example (b): There are several back-digitizations ξ and for some of them, the sequence of back-digitized bels does not form a semi-chain of $\mathcal{C}$. Example (c): There is a unique back-digitization ξ and the sequence of back-digitized bels does not form a semi-chain (for instance, the green points associated to the two pointed consecutive bels are not consecutive on the blue curve).

Definition 6 (Back-digitization) Let $\mathcal{C}$ be a Jordan curve and $h > 0$.

- A map $\mathrm{Bel}_h(\mathcal{C}) \to \mathcal{C}$ is called a *back-digitization* if for every bel $p \in \mathrm{Bel}_h(\mathcal{C})$, $\xi(p) \in p$
- A back-digitization $\xi\colon (b_i)_{i\in\mathbb{Z}/N\mathbb{Z}} \to \mathcal{C}$ is *monotonic* if $(\xi(b_i))_{i\in\mathbb{Z}/N\mathbb{Z}}$ is a semi-chain of $\mathcal{C}$.
- If $\mathcal{C}$ is a LTB curve, a back-digitization $\xi\colon (b_i)_{i\in\mathbb{Z}/N\mathbb{Z}} \to \mathcal{C}$ is a *monotonic sampler* if $(\xi(b_i))_{i\in\mathbb{Z}/N\mathbb{Z}}$ is a sampling semi-chain of $\mathcal{C}$.

As shown in Figure 12, there are curves with non-monotonic back-digitization or even, with no monotonic back-digitization. Nevertheless, in the sequel of Section 3, we prove the following proposition about the monotonicity of the sampling under LTB hypothesis.

Proposition 2 *Let $\mathcal{C}$ be a δ-LTB curve. On a compatible grid, any back-digitization is a monotonic sampler.*

The proof of Proposition 2 is split into three steps. In the first step, we prove that some configurations cannot appear in the digitization of a LTB curve (Subsection 3.2). In the second step, we define a specific back-digitization called the *canonical back-digitization* and prove it to be a monotonic sampler (Subsection 3.3). In the third step, we prove that any back-digitization of a LTB curve is a monotonic sampler (Subsection 3.4). In Subsection 3.5, given a back-digitization ξ, we prove that tight enough subsequences of $(\xi(b_i))_{i\in\mathbb{Z}/N\mathbb{Z}}$ are also sampling semi-chains.

3.2 Impossible configurations

The first step of the proof of the back-digitization monotonicity consists in excluding local configurations in the digitization of a LTB curve on a compatible grid (Lemma 5). In order to exclude these configurations, we use geometrical arguments based on the turn and, in particular, results about the T-straightest arc (Properties 8, 9, 10) and introduce Lemma 4 that precises Property 10 in the case where the square T is a BDP. Figure 13 illustrates the proof.

Lemma 4 *Let $\mathcal{C}$ be a δ-LTB Jordan curve. Let T be a* BDP *compatible with $\mathcal{C}$ and having a vertex v lying on $\mathcal{C}$. If v belongs to a bel of T, then the vertex v is an endpoint of the T-straightest arc of $\mathcal{C}$.*

Proof By contradiction, assume that v is not an end of the T-straightest arc $\boldsymbol{C}_T$. Then, by Property 10, the arc $\boldsymbol{C}_T$ is included in $[a, v, b]$ and its turn is equal to $\pi/2$ (see Figure 13). Let a and b be the two vertices of T adjacent to v. Let p, q be the ends of $\boldsymbol{C}_T$, $p \in (a, v)$ and $q \in (v, b]$. Since, by the compatibility hypothesis, the diameter of T is smaller than δ, there exist points close to p in $\mathcal{C} \setminus T$ at distance from q less than δ. Let p' be such a point (see Figure 13). On the one hand, the turn of the arc between p' and q including the arc $\boldsymbol{C}_T$ is greater than $\pi/2$. Thus, it is distinct from the straightest arc between p' and q. On the other hand, the straightest arc between p' and q is included in the disk whose diameter is $[p', q]$ (Property 4). Then, the diameter of the curve $\mathcal{C}$ is less than δ which contradicts Property 2. □

The purpose of the next lemma is to show that configurations depicted in Figure 14 cannot appear in the digitization of a LTB curve on a compatible grid. Notice that other configurations are already excluded by the well-composedness (Property 7).

Lemma 5 (Impossible configurations) *Let $\mathcal{C}$ be a δ-LTB curve. Given a grid compatible with $\mathcal{C}$, the configurations depicted in Figure 14 cannot appear in the digitization of $\mathcal{C}$.*

Proof For the first three configurations, let V be the square which is the union of the four BDP of the configuration. We define an orthonormal coordinate system

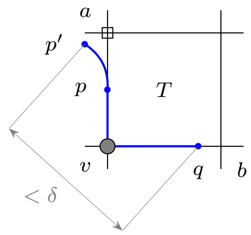

Figure 13: Grid square T with an exterior vertex (square) and a border vertex (circle). The configuration is described up to a rigid transformation preserving $h\mathbb{Z}^2$. Any arc containing the T-straightest arcwithout having p for end has its turn greater than $\frac{\pi}{2}$.

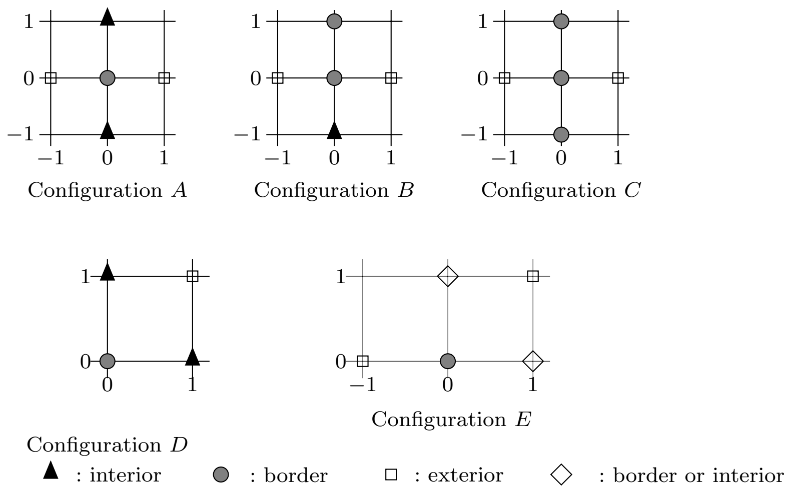

Figure 14: The configurations are defined up to a rigid transformation preserving $h\mathbb{Z}^2$.

by letting the center of V be the point $(0, 0)$ and the two exterior points be the points $(1, 0)$ and $(-1, 0)$. Notice that the border point $(0, 0)$ is an endpoint of each T-straightest arc of a dual pixel included in V (Lemma 4). Then, the union of the arcs passing through the four BDP is path connected.

– *Configuration A*. Let P be one of the four BDP included in V and p be the endpoint of $\boldsymbol{C}_P$ distinct from $(0, 0)$. The point p lies in the boundary of V for the segment $[(0, 0), p]$ separates the exterior vertex of P from the interior vertex of P (Property 9). Notice that the point p does not belong to the swelling of another BDP of V, since the arc passing through a BDP is included in the swelling of the BDP. Thereby, $\boldsymbol{C}_P$ is not included in another arc passing through a BDP of V. Then, four distinct arcs of $\mathcal{C}$ meet in $(0, 0)$ which contradicts the simplicity of the curve $\mathcal{C}$. Thus, on a LTB curve, Configuration A is impossible.

- *Configuration B*. Assume that the interior point has $(0,-1)$ for coordinates. On the one hand, the same arguments as in the first Configuration hold for the dual pixels $P_{(-0.5,-0.5)}$ and $P_{(0.5,-0.5)}$. On the other hand, the T-straightest arc of the dual pixel $P_{(-0.5,0.5)}$ is included in the swollen set of $P_{(-0.5,0.5)}$ and contains the vertex $(0,1)$. Hence, it is distinct from the arcs passing through $P_{(-0.5,-0.5)}$ and $P_{(0.5,-0.5)}$. Thus, three distinct arcs of $\mathcal{C}$ meet in $(0,0)$: on a LTB curve, Configuration B is impossible.
- *Configuration C*. From Properties 4, 10 and Lemma 4, the union $\boldsymbol{C}_{P_{(-0.5,0.5)}} \cup \boldsymbol{C}_{P_{(0.5,0.5)}}$ of the arcs passing through $P_{(-0.5,0.5)}$ and $P_{(0.5,0.5)}$ is an arc of $\mathcal{C}$ containing the points $(0,1)$ and $(0,0)$, and included in the union of the disk of diameter $[(0,1),(0,0)]$ with the segment $[(-1,1),(1,1)]$. Moreover, by Property 8, the intersection of $\mathcal{C}$ with $P_{(-0.5,0.5)} \cup P_{(0.5,0.5)}$ is included in $\boldsymbol{C}_{P_{(-0.5,0.5)}} \cup \boldsymbol{C}_{P_{(0.5,0.5)}}$. Alike, $\mathcal{C} \cap (P_{(-0.5,-0.5)} \cup P_{(0.5,-0.5)}) \subseteq \boldsymbol{C}_{P_{(-0.5,-0.5)}} \cup \boldsymbol{C}_{P_{(0.5,-0.5)}}$ is an arc of $\mathcal{C}$ passing through the points $(0,-1)$ and $(0,0)$, and included in the union of the disk of diameter $[(0,-1),(0,0)]$ with the segment $[(-1,-1),(1,-1)]$. Then, $\mathcal{C} \cap V$ is an arc of $\mathcal{C}$ that separates two exterior points in two distinct connected components of $\mathbb{R}^2 \setminus \mathcal{C}$: on a LTB curve, the configuration C is impossible.
- *Configuration D*. We define an orthonormal coordinate system by letting the border point having the coordinates $(0,0)$ and letting the exterior point having the coordinates $(1,1)$. By Property 9, one end of the $P_{(0.5,0.5)}$-straightest arc is on the open bel $((0,1),(1,1))$ and the other on the open bel $((1,0),(1,1))$. This contradicts Property 10. Thus, Configuration D never occurs on a LTB curve.
- *Configuration E*. We define an orthonormal coordinate system by letting the border point having the coordinates $(0,0)$, the border or interior points having the coordinates $(0,1)$ and $(1,0)$ and the two exterior points having coordinates $(-1,0)$ and $(1,1)$. Since Configuration D cannot occur, $(0,1)$ or $(1,0)$ is a border point. Let us show by contradiction that actually both points are border points. Assume for instance that $(1,0)$ is an interior point (exactly the same arguments hold for $(0,1)$). Then the curve $\mathcal{C}$ intersects the open bel $((1,0),(1,1))$ at a point f. By Lemma 4 $(0,1)$ is an end of the $P_{(0.5,0.5)}$-straightest arc. Then either $[(0,1),f,(0,0)]$ or $[(0,1),(0,0),f]$ is a chain of $\mathcal{C}$ included in the $P_{(0.5,0.5)}$-straightest arc. We derive that the $P_{(0.5,0.5)}$-straightest arc has its turn greater than $\frac{\pi}{2}$ which is absurd. Hence, $(0,1)$ and $(1,0)$ are both border points and, by Lemma 4 and Property 10, $\boldsymbol{C}_{P_{(0.5,0.5)}} = [(0,1),(0,0),(1,0)]$. Moreover, from Property 5, the intersection of the Jordan curve $\mathcal{C}$ with the closed set $B((0,0),h)$ equals the polygonal line $[(0,1),(0,0),(1,0)]$. Then the intersection of the Jordan curve $\mathcal{C}$ with the closed set $P_{(0.5,0.5)} \cup B((0,0),h)$ also equals the polygonal line $[(0,1),(0,0),(1,0)]$. We derive that the two exterior points shown in Configuration E lie in two different connected components of $P_{(0.5,0.5)} \cup B((0,0),h) \setminus [(0,1),(0,0),(1,0)]$. Thereby, the two exterior points shown in Configuration E lie in two distinct components of $\mathbb{R}^2 \setminus \mathcal{C}$ which contradicts the Jordan curve theorem. Hence, Configuration E cannot occur on a LTB curve. $\square$

3.3 The canonical back-digitization is a monotonic sampler

This subsection is devoted to the study of a particular back-digitization, the *canonical back-digitization*. Thanks to the lemmas established in Subsection 3.2, we will prove that the back-digitization is a monotonic sampler. Let us now define this canonical back-digitization.

Definition 7 (canonical back-digitization) Let $\mathcal{C}$ be a LTB curve and $(b_i)_{i\in\mathbb{Z}/N\mathbb{Z}}$ be a cyclically ordered set of its bels on a compatible grid. Denoting by T_i the BDP containing both b_i and b_{i+1}, the *canonical back-digitization* ξ_c associates to each b_i either the unique T_i-straightest arc endpoint lying on b_i or the one which is not a grid point.

The correctness of Definition 7 is a consequence of the next lemma.

Lemma 6 *Let $\mathcal{C}$ be δ-LTB curve and T be a* BDP *on a grid compatible with $\mathcal{C}$. The endpoints of the T-straightest arc $\boldsymbol{C}_T$ lie on the bels of T and conversely each bel of T contains an endpoint of $\boldsymbol{C}_T$. In particular, if both endpoints of $\boldsymbol{C}_T$ belong to a same bel, one of them is a grid point.*

Proof Let b be a bel of T and p_{in} be its inner-or-border point. If p_{in} is interior, then, from Property 9, b contains an end-point of $\boldsymbol{C}_T$. If p_{in} lies on $\mathcal{C}$, from Lemma 4, p_{in} is an end-point of $\boldsymbol{C}_T$. In the case where the two bels share their inner-or-border point which is an end-point of $\boldsymbol{C}_T$, Property 9 shows that no end-point of $\boldsymbol{C}_T$ lies on the two edges of T that are not bels. If both endpoints of $\boldsymbol{C}_T$ belong to b, one of them is shared with the other bel of T and therefore is a grid point. □

Since the digitization is well-composed, the mapping $b_i \mapsto T_i$ is a one-to-one correspondence between the bels and the BDPs. Nevertheless, the canonical back-digitization may not be one-to-one since consecutive images of ξ_c can be equal. For instance, a point of the curve lying on a grid point may yield three consecutive identical images (see Figure 10). The following proposition clarifies this possibility.

Proposition 1 *Let $\mathcal{C}$ be a LTB curve and $(b_i)_{i\in\mathbb{Z}/N\mathbb{Z}}$ be a cyclically ordered set of its bels on a compatible grid. Then, if for some i and j in $\mathbb{Z}/N\mathbb{Z}$, $\xi_c(b_j)$ lies on the straightest arc linking $\xi_c(b_i)$ and $\xi_c(b_{i+1})$, then either $j \in [\![i-2, i]\!]$ and $\xi_c(b_j) = \xi_c(b_i)$ or $j \in [\![i+1, i+3]\!]$ and $\xi_c(b_j) = \xi_c(b_{i+1})$.*

Proof Let $(b_i)_{i\in\mathbb{Z}/N\mathbb{Z}}$ be the cyclically ordered set of bels. Assume that $\xi_c(b_j)$ lies on the straightest arc linking $\xi_c(b_i)$ and $\xi_c(b_{i+1})$ for some $j \notin \{i, i+1\}$. Then, $\xi_c(b_j)$ belongs to the T_i-straightest arc where T_i is the BDP containing b_i and b_{i+1}. Hence, it belongs to the swelling of T_i. Since $\xi_c(b_j)$ lies on a bel, that is on an edge of the grid, actually, $\xi_c(b_j) \in T_i$. Since T_i is a BDP, T_i has at least an exterior point for vertex and, since the intersection of a bel $b_j \notin \{b_i, b_{i+1}\}$ with the BDP T_i is necessarily a vertex of the grid, the border point $\xi_c(b_j)$ is also a vertex of T_i. Let us prove that one of the bels b_i or b_{i+1} has $\xi_c(b_j)$ for end. By contradiction, assume that $\xi_c(b_j)$ is not an end of b_i nor of b_{i+1}. By well-composedness (Property 7), the BDP T_i has exactly two bels for edges. Then, the two edges of T_i having $\xi_c(b_j)$ for end are not bels. Therefore, their other end is also an interior point. The two other edges of T_i being bels, the vertex of T_i diagonally opposed to $\xi_c(b_j)$ is an exterior

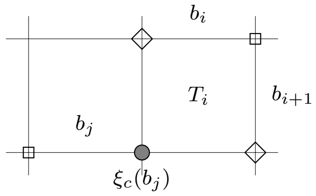

Figure 15: If neither of the bels b_i and b_{i+1} have $\xi_c(b_j)$ for end, then we recover Configuration E. The white squares correspond to exterior points, the gray disk to a point on $\mathcal{C}$, the white diamonds correspond to interior points or points on $\mathcal{C}$.

point. Since b_j is a bel, one of its end is an exterior point, then Configuration E occurs, which contradicts Lemma 5. Then one of the bels b_i or b_{i+1} has $\xi_c(b_j)$ for end. Then the border point $\xi_c(b_j)$ is a vertex of an edge of T_i having an exterior point for the other end, that is a vertex of b_i or b_{i+1}. We assume that $\xi_c(b_j) \in b_i$ (the case $\xi_c(b_j) \in b_{i+1}$ is similar). We derive from Lemma 4, that $\xi_c(b_j)$ is an endpoint of $\boldsymbol{C}_{T_i}$. Then, either $\xi_c(b_i) = \xi_c(b_j)$ or $\xi_c(b_j)$ is the second endpoint of the T_i-straightest arc (by definition of ξ_c). In the latter case, both endpoints of the T_i-straightest arc belong to b_i and $\boldsymbol{C}_{T_i}$ is included in the disk with diameter b_i (Property 4). Therefore, $\xi_c(b_{i+1})$, which lies in both b_{i+1} and the T_i-straightest arc is the intersection of b_{i+1} and the disk with diameter b_i which is the grid point $\xi_c(b_j)$ since the other endpoint of b_i is an exterior point. At this stage, we have proved that

1. either $\xi_c(b_j) = \xi_c(b_i)$ or $\xi_c(b_j) = \xi_c(b_{i+1})$.
2. $\xi_c(b_j)$ is a grid point.

Let b_k be one of the bels such that $\xi_c(b_k) = \xi_c(b_j)$ with $k \in \{i, i+1\}$. There are two possibilities: either b_k and b_j are orthogonal (Figure 16-a) or they are aligned (Figure 16-b).

In the first case, b_k and b_j are two orthogonal bels sharing a vertex, thus they share a BDP. Since there are exactly two bels per BDP, $|k - i| = 1$, moreover $j \notin \{i, i+1\}$, then either $k = i$ and $j = i - 1$ or $k = i + 1$ and $j = i + 2$.

In the second case b_k and b_j are aligned. We derive from Lemma 5 (Configurations A, B, C) that there is a third bel $b_{k'}$ having $\xi_c(b_j)$ as extremity. Then $|k - j| = 2$. Thus $j \in [\![i-2, i+3]\!]$. If $(k, j) = (i, i-2)$ or $(k, j) = (i+1, i+3)$, there is nothing left to prove since $\xi_c(b_k) = \xi_c(b_j)$. Otherwise, $(k, j) = (i, i+2)$ or $(k, j) = (i+1, i-1)$. It remains to prove that $\xi_c(b_{i+2}) = \xi_c(b_{i+1})$ or $\xi_c(b_{i-1}) = \xi_c(b_i)$. Assume that $(k, j) = (i, i+2)$ (the case $(k, j) = (i+1, i-1)$ is similar) and, by contradiction, that $\xi_c(b_{i+1}) \neq \xi_c(b_j)$. By Lemma 4, $\xi_c(b_j)$ is an endpoint of the T_{i+1}-straightest arc. Therefore, from the assumptions and the definition of ξ_c, all the endpoints of the T_i-straightest arc and the T_{i+1}-straightest arc are in b_{i+1}. Then, by Property 4, $\boldsymbol{C}_{T_i} \cup \boldsymbol{C}_{T_{i+1}}$ is included in the disk D with diameter $[\xi_c(b_j), q]$ where q is the exterior point of the bel b_{i+1} (see Figure 16-c). We have a contradiction with the simplicity of $\mathcal{C}$ and the fact that the arc $\mathcal{C} \setminus (\boldsymbol{C}_{T_i} \cup \boldsymbol{C}_{T_{i+1}})$ does not intersect $T_i \cup T_{i+1}$ (Property 8). $\square$

Proposition 1 is the heart of the proof of the monotonicity of the canonical back-digitization. Corollary 1 is only a formal verification that the result of Proposition 1 coincides with the definition of the monotonicity.

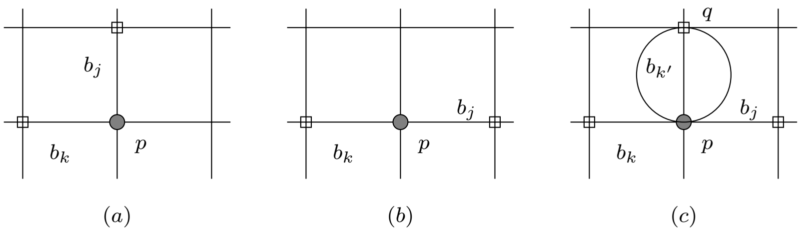

Figure 16: (Proof of Proposition 1) The bels b_j and b_k share the same image p by the canonical back-digitization ξ_c.

Corollary 1 *Let $\mathcal{C}$ be a LTB curve and $(b_i)_{i\in\mathbb{Z}/N\mathbb{Z}}$ be a cyclically ordered set of its bels on a compatible grid. The canonical back-digitization is a monotonic sampler.*

Proof In this proof, the cardinal of a subsequence $(\xi_c(b_k))_{k\in[\![i,j]\!]}$ of $(\xi_c(b_i))_{i\in\mathbb{Z}/N\mathbb{Z}}$ $(i, j \in \mathbb{Z}/N\mathbb{Z})$, is the cardinal of the set $\{\xi_c(b_k)\}_{k\in[\![i,j]\!]}$ and we set $M = \#\xi_c(\mathrm{Bel}_h(\mathcal{C}))$ (Since ξ_c is not injective, M does not need be equal to N). We assume $M \geq 3$ (otherwise, the result is obvious).

Let us firstly prove that $(\xi_c(b_i))_{i\in\mathbb{Z}/N\mathbb{Z}}$ is a semi-chain. For any $n \in [2, M/2+1] \cap \mathbb{N}$, let H_n be the induction hypothesis: "for any $i, j \in \mathbb{Z}/N\mathbb{Z}$ and any subsequence $(\xi_c(b_k))_{k\in[\![i,j]\!]}$ of $(\xi_c(b_i))_{i\in\mathbb{Z}/N\mathbb{Z}}$ whose cardinal is less than n, the two sets resulting from the intersection of the closed arcs from $\xi_c(b_i)$ to $\xi_c(b_j)$ with $\xi_c(\mathrm{Bel}_h(\mathcal{C}))$ are equal to $\{\xi_c(b_k)\}_{k\in[\![i,j]\!]}$ and $\{\xi_c(b_k)\}_{k\in[\![j,i]\!]}$" . Notice that between any two terms of the sequence $(\xi_c(b_i))_{i\in\mathbb{Z}/N\mathbb{Z}}$ there is an arc containing at most $\lfloor M/2+1\rfloor$ terms of the sequence. Hence $H_{\lfloor M/2+1\rfloor}$ states that $(\xi_c(b_i))_{i\in\mathbb{Z}/N\mathbb{Z}}$ is a semi-chain.

– (Case n=2) From Proposition 1, we get that, for any $i \in \mathbb{Z}/N\mathbb{Z}$, the intersections of the closed arcs from $\xi_c(b_i)$ to $\xi_c(b_{i+1})$ with $\xi_c(\mathrm{Bel}_h(\mathcal{C}))$ are equal to $\{\xi_c(b_k)\}_{k\in[\![i,i+1]\!]}$ (for the straightest arc) and $\{\xi_c(b_k)\}_{k\in[\![i+1,i]\!]}$ (for the complementary arc). It is plain that we can extend this property to closed arcs from $\xi_c(b_i)$ to $\xi_c(b_j)$ provided that either $\#\{\xi_k\}_{k\in[\![i,j]\!]} \leq 2$ or $\#\{\xi_k\}_{k\in[\![j,i]\!]} \leq 2$. Then H_2.

– Let $n \geq 3$. Assume H_{n-1}. We consider two integers i and j in $\mathbb{Z}/N\mathbb{Z}$ such that $\#\{\xi_c(b_k)\}_{k\in[\![i,j]\!]} = n$. There exists $\ell \in [\![i,j]\!]$ such that $\#\{\xi_c(b_k)\}_{k\in[\![i,\ell]\!]} = n-1$ and $\#\{\xi_c(b_k)\}_{k\in[\![i,\ell+1]\!]} = n$. We write $C_{i,\ell}$, resp. $C_{\ell,i}$, for the arc between $\xi_c(b_i)$ and $\xi_c(b_\ell)$ whose intersection with $\mathrm{Bel}_h(\mathcal{C})$ is equal to $\{\xi_c(b_k)\}_{k\in[\![i,\ell]\!]}$, resp. $\{\xi_c(b_k)\}_{k\in[\![\ell,i]\!]}$ (we use the induction hypothesis H_{n-1}). Since $\xi_c(b_{\ell+1}) \notin \{\xi_c(b_k)\}_{k\in[\![i,\ell]\!]}$ (by definition of ℓ), $\xi_c(b_{\ell+1})$ lies in the interior of $C_{\ell,i}$. Furthermore, by Proposition 1, the open straightest arc $\mathring{\boldsymbol{C}}_{\xi_c(b_\ell),\xi_c(b_{\ell+1})}$ from $\xi_c(b_\ell)$ to $\xi_c(b_{\ell+1})$ does not contain any point of $\xi_c(\mathrm{Bel}_h(\mathcal{C}))$. Then, $C_{i,\ell+1} := C_{i,\ell} \sqcup \mathring{\boldsymbol{C}}_{\xi_c(b_\ell),\xi_c(b_{\ell+1})} \sqcup \{\xi_c(b_{\ell+1})\}$ is an arc from $\xi_c(b_i)$ to $\xi_c(b_{\ell+1})$ whose intersection with $\xi_c(\mathrm{Bel}_h(\mathcal{C}))$ is $\{\xi_c(b_k)\}_{k\in[\![i,\ell+1]\!]}$.

Alike, the arc $C_{\ell,i} \setminus (\{\xi_c(b_\ell)\} \sqcup \mathring{\boldsymbol{C}}_{\xi_c(b_\ell),\xi_c(b_{\ell+1})})$ is an arc from $\xi_c(b_i)$ to $\xi_c(b_{\ell+1})$ whose intersection with $\xi_c(\mathrm{Bel}_h(\mathcal{C}))$ is $\{\xi_c(b_k)\}_{k\in[\![\ell+1,i]\!]}$. It remains to show that the points $\xi_c(b_k)$, $k \in [\![l+1, j]\!]$, are all equal to $\xi_c(b_{l+1})$ (indeed $\xi_c(b_k)$, with $k \in [\![l+1, j]\!]$, could be equal to a $\xi_c(b_m)$ for some $m \in [\![i, l]\!]$). For any $k \in [\![l+1, j]\!]$, let P_k be the induction hypothesis :" $\xi(b_k) = \xi(b_{l+1})$".

  – P_{l+1} is obvious.

– Let $k \in [\![l+2, j]\!]$, assume P_{l+1}, ..., P_{k-1}, i.e. $\xi_c(b_{\ell+1}) = \xi_c(b_{\ell+2}) = \cdots = \xi_c(b_{k-1})$.
  - By definition of ℓ, $\xi_c(b_k) \in C_{i,\ell+1}$ and $\xi_c(b_k) \in C_{\ell,i}$. Then,

$$\begin{aligned}\xi_c(b_k) &\in C_{i,\ell+1} \cap C_{\ell,i} \cap \xi_c(\mathrm{Bel}_h(\mathcal{C})),\\ &= (C_{i,\ell} \sqcup \mathring{\boldsymbol{C}}_{\xi_c(b_\ell),\xi_c(b_{\ell+1})} \sqcup \{\xi_c(b_{\ell+1})\}) \cap C_{\ell,i} \cap \xi_c(\mathrm{Bel}_h(\mathcal{C})),\\ &= (C_{i,l} \cap C_{l,i} \cap \xi_c(\mathrm{Bel}_h(\mathcal{C}))) \sqcup \{\xi_c(b_{l+1})\},\\ &= \{\xi(b_i), \xi(b_l), \xi(b_{l+1})\}.\end{aligned}$$

  - By contradiction assume that $\xi_c(b_k) = \xi_c(b_\ell)$. Then, on the one hand, one of the arc between $\xi_c(b_\ell)$ and $\xi_c(b_k)$ is a singleton while the other arc is $\mathcal{C}$. On the other hand, by the induction hypothesis H_{n-1}, one of the arcs between $\xi_c(b_\ell)$ and $\xi_c(b_k)$ contains exactly two points of $\xi_c(\mathrm{Bel}_h(\mathcal{C}))$, $\xi_c(b_\ell)$ and $\xi_c(b_{\ell+1})$. It follows that the cardinal of $\xi_c(\mathrm{Bel}_h(\mathcal{C}))$ is 2 which contradicts the assumption $M \geq 3$. Thus, $\xi_c(b_k) \neq \xi_c(b_\ell)$.
  - By contradiction assume that $\xi_c(b_k) = \xi_c(b_i)$. Then, on the one hand, one of the arcs between $\xi_c(b_{\ell+1})$ and $\xi_c(b_k)$ is $C_{i,\ell+1}$. By definition of l, this arc contains exactly n points of $\xi_c(\mathrm{Bel}_h(\mathcal{C}))$ where $n \geq 3$. On the other hand, by the induction hypothesis P_{k-1}, one of the arcs between $\xi_c(b_{\ell+1})$ and $\xi_c(b_k)$ contains at most two points of $\xi_c(\mathrm{Bel}_h(\mathcal{C}))$ while the other arc contains all the points of $\xi_c(\mathrm{Bel}_h(\mathcal{C}))$. It follows that the cardinal of $\xi_c(\mathrm{Bel}_h(\mathcal{C}))$ is n which contradicts the assumptions $n \leq M/2+1$ and $M \geq 3$. Then, $\xi_c(b_k) \neq \xi_c(b_i)$. Since $\xi_c(b_k) \in \{\xi_c(b_i), \xi_c(b_l), \xi_c(b_{l+1})\}$, P_k.

  Finally, we derive that $\xi_c(b_{\ell+1}) = \xi_c(b_{\ell+2}) = \ldots = \xi_c(b_j)$.

Then, $C_{i,\ell+1}$ is an arc from $\xi_c(b_i)$ to $\xi_c(b_j)$ whose intersection with $\xi_c(\mathrm{Bel}_h(\mathcal{C}))$ is $\{\xi_c(b_k)\}_{k\in[\![i,j]\!]}$. Alike, the arc $C_{\ell,i} \setminus (\{\xi_c(b_\ell)\} \sqcup \mathring{\boldsymbol{C}}_{\xi_c(b_\ell),\xi_c(b_{\ell+1})})$ is an arc from $\xi_c(b_i)$ to $\xi_c(b_j)$ whose intersection with $\xi_c(\mathrm{Bel}_h(\mathcal{C}))$ is $\{\xi_c(b_k)\}_{k\in[\![j,i]\!]}$. Then H_n.

Eventually, observe that the sequence $(\xi_c(b_k))_{k\in\mathbb{Z}/N\mathbb{Z}}$ is a sampling semi-chain. Indeed, $\mathrm{d}(b_k, b_{k+1}) < \delta$ for any k because the grid is compatible with $\mathcal{C}$ and the straightest arc between $\xi_c(b_k)$ and $\xi_c(b_{k+1})$ does not contain any point of $\xi_c(\mathrm{Bel}_h(\mathcal{C}))$ by Proposition 1. □

3.4 Any back-digitization is a monotonic sampler

We now show that any back-digitization defined on the bel set of a LTB curve is a monotonic sampler. The heart of this result is brought by the following lemma.

Lemma 7 *Let $\mathcal{C}$ be a LTB curve and $(b_i)_{i\in\mathbb{Z}/N\mathbb{Z}}$ be a cyclically ordered set of its bels on a compatible grid. Let ξ be a back-digitization. Then, for any $i \in \mathbb{Z}/N\mathbb{Z}$, $\xi(b_i)$ lies on the straightest arc between $\xi_c(b_i)$ and $\xi_c(b_{i+1})$.*

Proof Let T_i, resp. T_{i+1}, be the BDP containing both b_i and b_{i+1}, resp. b_{i+1} and b_{i+2}. By definition of a back-digitization, $\xi(b_i) \in b_i$ and $\xi_c(b_{i+1}) \in b_{i+1}$. Then, $\xi(b_i)$ and $\xi_c(b_{i+1})$ lie on $\boldsymbol{C}_{T_i}$, the T_i -straightest arc. Recall that, by definition of ξ_c, $\xi_c(b_i)$ is an endpoint of $\boldsymbol{C}_{T_i}$ and that, by Lemma 6, e_i, the other end-point of $\boldsymbol{C}_{T_i}$, lies on b_{i+1}. By contradiction assume that $\xi(b_i)$ does not belong to the straightest arc between $\xi_c(b_i)$ and $\xi_c(b_{i+1})$. Then $\xi_c(b_{i+1}) \neq e_i$ and $\xi(b_i)$ belongs to the straightest arc between $\xi_c(b_{i+1})$ and e_i. This straightest arc is included in the disk with diameter $[\xi_c(b_{i+1}), e_i]$ (Property 4) which is itself included in the disk with diameter b_{i+1}. We derive that $\xi(b_i)$ is a grid point ($\{\xi(b_i)\} = b_i \cap b_{i+1}$) and, by Lemma 4, it is an end-point of $\boldsymbol{C}_{T_i}$, that is $\xi(b_i) = e_i$. Since both endpoints of $\boldsymbol{C}_{T_i}$ lie on b_i, $\boldsymbol{C}_{T_i}$ is included in the disk with diameter b_i and $\xi_c(b_{i+1}) = \xi(b_i)$. Contradiction! We conclude that $\xi(b_i)$ is in the straightest arc between $\xi_c(b_i)$ and $\xi_c(b_{i+1})$. $\square$

Establishing the monotony of a back-digitization needs further tedious calculations that will be carried out in Proposition 2. But before that, we still have to give a technical lemma about subsequences of semi-chains. This lemma is also of primary importance for the next subsection dealing with sparse samplings of a curve.

Lemma 8 *Let $\mathcal{C}$ be a δ-LTB curve.*

(a) Let a, b, c be three points of $\mathcal{C}$ such that $\mathrm{d}(a,b) < \delta$ and $\mathrm{d}(b,c) < \delta$. Let consider the three arcs such that $\mathcal{C} \setminus \{a,b,c\}$ is a disjoint union of these three arcs. Then one of them has its turn greater than $\frac{\pi}{2}$.

(b) Let $(a_k)_{k \in \mathbb{Z}/N\mathbb{Z}}$, $N \geq 3$, be a semi-chain of $\mathcal{C}$ such that, for any $i, j \in \mathbb{Z}/N\mathbb{Z}$, $\mathrm{d}(a_i, a_j) < \delta$ and, for any $k \in \mathbb{Z}/N\mathbb{Z} \setminus \{0\}$, the arc from a_{k-1} to a_k whose intersection with the semi-chain is $\{a_{k-1}, a_k\}$ is a straightest arc. Then, the arc from a_0 to a_{N-1} passing through $a_1, \ldots, a_{N-2}$ is a straightest arc.

Proof

(a) Let A be the arc of $\mathcal{C}$ between the points a and b and not containing the point c. If A is not a straightest arc, then by applying Fenchel's Theorem (the turn of closed curve is bounded from below by 2π) and the additivity of turns, both stated in Property 1, one has

$$\kappa(A) + < e_l(a), e_r(a) > + \kappa(\boldsymbol{A'}) + < e_l(b), e_r(b) > \geq 2\pi,$$

where $\boldsymbol{A'}$ is the straightest arc between a and b ($\boldsymbol{A'}$ exists for $\mathrm{d}(a,b) < \delta$). Moreover, from Lemma 1-b, we have

$$< e_l(a), e_r(a) > + \kappa(\boldsymbol{A'}) + < e_l(b), e_r(b) > \leq \frac{\pi}{2}.$$

Then $\kappa(A) \geq 2\pi - \pi/2 > \pi/2$ and we are done. The same arguments hold for the arc B between the points b and c and not containing the point a. Finally, if A and B are straightest arcs, we denote by C the arc of $\mathcal{C}$ between the points a and c and not containing the point b. Using as above Fenchel's Theorem, the additivity of turns and Lemma 1-b, we get

$$\begin{aligned}
\kappa(C) &\geq 2\pi - \big(< e_l(a), e_r(a) > + \kappa(A) + < e_l(b), e_r(b) > + \kappa(B) \\
&\qquad\qquad + < e_l(c), e_r(c) > \big) \\
&\geq 2\pi - \big(< e_l(a), e_r(a) > + \kappa(A) + < e_l(b), e_r(b) > \big) \\
&\qquad - \big(< e_l(b), e_r(b) > + \kappa(B) + < e_l(c), e_r(c) > \big) \\
&\geq 2\pi - \pi/2 - \pi/2 \\
&\geq \pi.
\end{aligned}$$

So, the result holds.

(b) The proof is done by finite induction on N.

If $N = 3$, the first part of this lemma permit us to derive that the arc of $\mathcal{C}$ between a_0 and a_2 and not containing a_1 has a turn greater than $\pi/2$ from the hypotheses of statement (b):

(*i*) the turn of the arc between a_0 and a_1 not containing a_2 is not greater than $\pi/2$,

(*ii*) the turn of the arc between a_1 and a_2 not containing a_0 is not greater than $\pi/2$.

Then, the straightest arc between a_0 and a_2 which exists for $\mathrm{d}(a_0, a_2) < \delta$, is the arc between a_0 and a_2 and containing a_1.

Assume that the result holds for the semi-chain $(a_k)_{k\in[\![0,n]\!]}$ where $3 \leq n \leq N-1$. On the one hand, from the induction hypothesis, the arc C_n between a_0 and a_n not containing a_N is a straightest arc. On the other hand, from the general hypothesis, the arc from a_n to a_{n+1} not containing a_0 is a straightest arc. Then, from the first part of this lemma, the arc from a_{n+1} to a_0 not containing the points a_i, $1 \leq i \leq n$, has a turn greater than $\pi/2$. Thus, this arc cannot be a straightest arc though such a straightest arc between a_0 and a_{n+1} exists (for $\mathrm{d}(a_0, a_{n+1}) < \delta$). We conclude that the arc from a_0 to a_{n+1} passing through $a_i, \ldots, a_n$ is a straightest arc. This achieves the induction □

Eventually, thanks to Lemmas 3,7 and 8, we can now state the result announced at the beginning of this section and recalled here :

Proposition 2 *Let $\mathcal{C}$ a δ-LTB curve. On a compatible grid, any back-digitization is a monotonic sampler.*

Proof Let $(b_i)_{i\in\mathbb{Z}/N\mathbb{Z}}$ be a cyclically ordered set of the bels associated to $\mathcal{C}$ on a compatible grid and ξ be a back-digitization. Let $i, j \in \mathbb{Z}/N\mathbb{Z}$. We consider the following sets:

$$C_1 = \{\xi_c(b_k)\}_{k\in[\![i,j+1]\!]} \sqcup \bigsqcup_{k\in[\![i,j]\!]} \mathring{\boldsymbol{C}}_{\xi_c(b_k),\xi_c(b_{k+1})},$$

and

$$C_2 = \{\xi_c(b_k)\}_{k\in[\![j,i+1]\!]} \sqcup \bigsqcup_{k\in[\![j,i]\!]} \mathring{\boldsymbol{C}}_{\xi_c(b_k),\xi_c(b_{k+1})}.$$

From Lemma 3, C_1 is an arc between $\xi_c(b_i)$ and $\xi_c(b_{j+1})$ and C_2 is an arc between $\xi_c(b_j)$ and $\xi_c(b_{i+1})$. From Lemma 7, we derive that

$$C_1 = \bigsqcup_{k\in[\![i,j]\!]} \left(\mathring{\boldsymbol{C}}_{\xi_c(b_k),\xi(b_k)} \sqcup \mathring{\boldsymbol{C}}_{\xi(b_k),\xi_c(b_{k+1})}\right) \sqcup \{\xi(b_k)\}_{k\in[\![i,j]\!]} \sqcup \left(\{\xi_c(b_k)\}_{k\in[\![i,j+1]\!]} \setminus \{\xi(b_k)\}_{k\in[\![i,j]\!]}\right), \quad (1)$$

and

$$C_2 = \bigsqcup_{k\in[\![j,i]\!]} \left(\mathring{\boldsymbol{C}}_{\xi_c(b_k),\xi(b_k)} \sqcup \mathring{\boldsymbol{C}}_{\xi(b_k),\xi_c(b_{k+1})}\right) \sqcup \{\xi(b_k)\}_{k\in[\![j,i]\!]} \sqcup \left(\{\xi_c(b_k)\}_{k\in[\![j,i+1]\!]} \setminus \{\xi(b_k)\}_{k\in[\![j,i]\!]}\right). \quad (2)$$

Lemma 8-b, applied to the semi-chains $(\xi(b_k), \xi_c(b_{k+1}), \xi(b_{k+1}))$, shows that the arcs $\mathring{\boldsymbol{C}}_{\xi(b_k),\xi_c(b_{k+1})} \sqcup \{\xi_c(b_{k+1})\} \sqcup \mathring{\boldsymbol{C}}_{\xi_c(b_{k+1}),\xi(b_{k+1})}$ are straightest arcs of $\mathcal{C}$, that is, $\mathring{\boldsymbol{C}}_{\xi(b_k),\xi(b_{k+1})} = \mathring{\boldsymbol{C}}_{\xi(b_k),\xi_c(b_{k+1})} \sqcup \{\xi_c(b_{k+1})\} \sqcup \mathring{\boldsymbol{C}}_{\xi_c(b_{k+1}),\xi(b_{k+1})}$. Observe that, if for some $k \in [\![i,j]\!]$, $\xi_c(b_{k+1}) \notin \{\xi_c(b_m)\}_{m\in[\![i,j+1]\!]} \setminus \{\xi(b_m)\}_{m\in[\![i,j]\!]}$, then $\xi_c(b_{k+1}) \in \{\xi(b_m)\}_{m\in[\![i,j]\!]}$ and since $\xi_c(b_{k+1}) \in \mathring{\boldsymbol{C}}_{\xi(b_k),\xi(b_{k+1})}$, $\xi_c(b_{k+1}) = \xi(b_k)$ or $\xi_c(b_{k+1}) = \xi(b_{k+1})$ and $\mathring{\boldsymbol{C}}_{\xi(b_k),\xi(b_{k+1})} = \mathring{\boldsymbol{C}}_{\xi_c(b_{k+1}),\xi(b_{k+1})}$ or $\mathring{\boldsymbol{C}}_{\xi(b_k),\xi(b_{k+1})} = \mathring{\boldsymbol{C}}_{\xi_c(b_k),\xi(b_{k+1})}$.The same reasoning holds if $\xi_c(b_{k+1}) \notin \{\xi_c(b_m)\}_{m\in[\![j,i+1]\!]} \setminus \{\xi(b_m)\}_{m\in[\![j,i]\!]}$. Then, Equations (1), (2) can be rewritten as

$$C_1 = \{\xi_c(b_i)\} \sqcup \mathring{\boldsymbol{C}}_{\xi_c(b_i),\xi(b_i)} \sqcup \left(\{\xi(b_k)\}_{k\in[\![i,j]\!]} \sqcup \bigsqcup_{k\in[\![i,j-1]\!]} \mathring{\boldsymbol{C}}_{\xi(b_k),\xi(b_{k+1})} \right) \sqcup \mathring{\boldsymbol{C}}_{\xi(b_j),\xi_c(b_{j+1})} \sqcup \{\xi_c(b_{j+1})\}$$

and

$$C_2 = \{\xi_c(b_j)\} \sqcup \mathring{\boldsymbol{C}}_{\xi_c(b_j),\xi(b_j)} \sqcup \left(\{\xi(b_k)\}_{k\in[\![j,i]\!]} \sqcup \bigsqcup_{k\in[\![j,i-1]\!]} \mathring{\boldsymbol{C}}_{\xi(b_k),\xi(b_{k+1})} \right) \sqcup \mathring{\boldsymbol{C}}_{\xi(b_i),\xi_c(b_{i+1})} \sqcup \{\xi_c(b_{i+1})\}.$$

Eventually, the latter equalities show that the arcs of $\mathcal{C}$ from $\xi(b_i)$ to $\xi(b_j)$ are

$$C'_1 = \bigsqcup_{k\in[\![i,j-1]\!]} \mathring{\boldsymbol{C}}_{\xi(b_k),\xi(b_{k+1})} \sqcup \{\xi(b_k)\}_{k\in[\![i,j]\!]} \tag{3}$$

and

$$C'_2 = \bigsqcup_{k\in[\![j,i-1]\!]} \mathring{\boldsymbol{C}}_{\xi(b_k),\xi(b_{k+1})} \sqcup \{\xi(b_k)\}_{k\in[\![j,i]\!]}. \tag{4}$$

Since $\mathcal{C}'_1$ and $\mathcal{C}'_2$ are complementary arcs, it can be seen that these two arcs intersect $\xi(\mathrm{Bel}_h(\mathcal{C}))$ respectively in $\{\xi(b_k)\}_{k\in[\![i,j]\!]}$ and $\{\xi(b_k)\}_{k\in[\![j,i]\!]}$. In particular, taking $j = i+1$, we see that the straightest arc between $\xi(b_i)$ and $\xi(b_{i+1})$ does not contain any point of $\xi(\mathrm{Bel}_h(\mathcal{C}))$ in its interior. Besides, by definition of a back-digitization, and since the grid is compatible with the curve $\mathcal{C}$, we have $\mathrm{d}(\xi(b_k), \xi(b_{k+1}) < \delta$ for any $k \in \mathbb{Z}/N\mathbb{Z}$. □

3.5 Sparse monotonic samplers

In this subsection, we extend Proposition 2 to subsequences of $\mathrm{Bel}_h(\mathcal{C})$ provided the back-digitization still yields sampling semi-chains. This is of interest for the length estimation where estimators should only use sparse subsequences of $\mathrm{Bel}_h(\mathcal{C})$ to be convergent (see Section Introduction).

Theorem 1 *Let $\mathcal{C}$ be a δ-LTB curve on a compatible grid $h\mathbb{Z}^2$. Let $\xi : \mathrm{Bel}_h(\mathcal{C}) \to \mathcal{C}$ be a back-digitization. Denoting by $(b_k)_{k\in\mathbb{Z}/N\mathbb{Z}}$ the cyclically ordered set $\mathrm{Bel}_h(\mathcal{C})$ and assuming $N \geq 3$, let $(b_{\sigma(i)})_{i\in\mathbb{Z}/N_\sigma\mathbb{Z}}$ be a subsequence of (b_k) such that $h\#[\![\sigma(i), \sigma(i+1)]\!] < \delta$. Then,*

$$\mathcal{C} = \bigcup_{i\in\mathbb{Z}/N_\sigma\mathbb{Z}} \boldsymbol{C}'_i,$$

where $\boldsymbol{C}'_i$ is the straightest arc between $\xi(b_{\sigma(i)})$ and $\xi(b_{\sigma(i+1)})$, and the intersection between $\boldsymbol{C}'_i$ and $\boldsymbol{C}'_j$ with $i \neq j$ is either empty or reduced to a point.

Proof In this proof, we write m_i for the middle of the bel b_i. For any $i \in \mathbb{Z}/N\mathbb{Z}$, let $\boldsymbol{C}_i$ be the straightest arc between $\xi(b_i)$ and $\xi(b_{i+1})$. From Proposition 2 , we have $\mathcal{C} = \bigcup_{i\in\mathbb{Z}/N\mathbb{Z}} \boldsymbol{C}_i$ with $\boldsymbol{C}_i \cap \boldsymbol{C}_j = \emptyset$ if $j - i \notin \{-1, 0, 1\}$ and $\boldsymbol{C}_i \cap \boldsymbol{C}_j$ is a singleton if $j - i \in \{-1, 1\}$.

Thus, $\mathcal{C} = \bigcup_{i\in\mathbb{Z}/N_\sigma\mathbb{Z}} C'_i$ where C'_i is defined by $C'_i = \bigcup_{j=\sigma(i)}^{\sigma(i+1)-1} \boldsymbol{C}_j$. Therefore, it is sufficient to prove that, for any $i \in \mathbb{Z}/N_\sigma\mathbb{Z}$, C'_i is a straightest arc. So, let $i \in \mathbb{Z}/N_\sigma\mathbb{Z}$. As $\#[\![\sigma(i), \sigma(i+1)]\!] < \delta/h$ and the d_1 distance (Manhattan distance) between two consecutive middles m_i and m_{i+1} is equal to h, the d_1 distance between any points m_j and m_k where $\sigma(i) \leq j < k \leq \sigma(i+1)$ is bounded from above by $\delta - h$. Moreover, by definition of a back-digitization, $|\xi(b_j) - m_j| \leq h/2$ for any $j \in [\![\sigma(i), \sigma(i+1)]\!]$. Hence, $d_1\big(\xi(b_j), \xi(b_k)\big) < \delta$ if $\sigma(i) \leq j < k \leq \sigma(i+1)$. Then, the Euclidean distance between $\xi(b_j)$ and $\xi(b_k)$ is also bounded from above by δ. All the assumptions of Lemma 8-(b) are then satisfied. Thereby, thanks to this lemma, we conclude that $\mathcal{C}'_i$ is a straightest arc and we are done. □

In Theorem 1, the expression $h\#[\![\sigma(i), \sigma(i+1)]\!]$ can be viewed as the d_1 length of the boundary polyline associated to the dual representation of the bels b_k, $k \in [\![\sigma(i), \sigma(i+1)]\!]$ (see Figure 17).

In the sequel, given a LTB curve $\mathcal{C}$ and a grid step h compatible with $\mathcal{C}$, any subsequence $(b_{\sigma(i)})_{i\in\mathbb{Z}/N_\sigma\mathbb{Z}}$ of the cyclically ordered sequence $(b_k)_{k\in\mathbb{Z}/N\mathbb{Z}}$ of the bels of the digitization of $\mathcal{C}$ is called a *normal subsequence of* $\mathrm{Bel}_h(\mathcal{C})$ if, for any $i \in \mathbb{Z}/N_\sigma\mathbb{Z}$, $(\#[\![\sigma(i+1), \sigma(i)]\!])h < \delta$.

4 Application to length estimation

It is well-known that the length of a rectifiable curve can be approximated with any arbitrary precision by the length of an inscribed polygonal line provided the polygonal edge lengths are small enough. This is no more true when the vertices of the polygonal line are rounded as explained in the introduction of this article. Thanks to the notion of monotonic sampler introduced in Section 3, we can now study the conditions under which the lengths of a grid polygon sequence converge towards the length of a LTB curve and with what speed. In this section, given a rectifiable curve $\mathcal{C}$, we denote by $\mathcal{L}(C)$ its length and given a positive integer n and a polygon P, we denote by $M_n(P)$ the mean, relying on the L_n norm, of the edge lengths of P:

$$M_n(P) = \left(\frac{1}{N}\sum_{k=0}^{N-1} {x_k}^n\right)^{\frac{1}{n}} \quad \text{if } n < \infty \quad \text{and} \quad M_\infty(P) = \sup_k(|x_k|),$$

where the real x_k are the edge lengths of P.

The difference between the true length of a curve and the length of a grid polygon is the sum of two discrepancies. The first one is the discrepancy between the length of the curve and the length of a polygon which is inscribed in the curve. This discrepancy is upper-bounded in Section 4.1. The second discrepancy, between the length of the inscribed polygon and the length of the grid polygon, is taken into account in Section 4.2 which concludes the study. The back-digitization defined in Section 3 permits us to put in correspondence the edges of the inscribed polygon and those of the grid polygon, and then to compare their lengths.

4.1 LTB curve length estimation using inscribed polygon

According to Jordan's definition of curve length, we compare the length of a LTB curve with the length of an inscribed polygon (without any rounding). More specifically, we focus on the convergence of the length of polygons inscribed in a LTB curve.

Given a LTB curve $\mathcal{C}$, we say that a polygon inscribed in $\mathcal{C}$ *splits* $\mathcal{C}$ *into straightest arcs* if the sequence of the vertices of the polygon is a sampling semi-chain of $\mathcal{C}$.

4.1.1 Turn and length

Intuitively, the more a curve of fixed length turns, the less it moves away from its origin. This is quantified in the following property.

Property 11 ([1], Theorem 5.8.1 p. 151) Let $\mathcal{C}$ be a curve such that $\kappa(\mathcal{C}) < \pi$ and let d be the distance between the ends of $\mathcal{C}$. Then,

$$\cos\left(\frac{\kappa(\mathcal{C})}{2}\right) \times \mathcal{L}(\mathcal{C}) \leq d.$$

Notice that this bound is sharp and the equality case only holds for a polygonal line of two sides of same length [1].

4.1.2 General case

Here, we study the general case of a LTB-curve without smoothness assumption. The difference in length between the curve $\mathcal{C}$ and the inscribed polygon L_k is split into two parts. The first part $(\frac{M_\infty(L_k)^{2\mu}}{M_1(L_k)^{1/2}})$ bounds the difference in length between the arcs of smaller turns and the chords joining their ends. The second part $(M_\infty(L_k)^{1-\mu})$ bounds the difference in length between the arcs of greater turns and their chords. The first part converges thanks to the hypothesis $M_\infty(L_k)^{4\mu} = o\,(M_1(L_k))$ as $k \to +\infty$. The second part converges since the number of arcs of great turn decreases relatively to the total number of arcs. The parameter μ discriminates the arcs of small turn and great turn. The convergence hypothesis $M_\infty(L_k)^{4\mu} = o\,(M_1(L_k))$ constrains the choice of the parameter μ. It restricts the discrepancy of the rate of convergence of the different edges of L_k (there should not be any edge length tending toward 0 too slowly in comparison with the other edge lengths).

Proposition 3 *Let $\mathcal{C}$ be a δ-LTB curve with $\delta > 0$. Let (L_k) be a sequence of polygons splitting the curve into straightest arcs. Assume $\lim_{k\to+\infty} M_1(L_k) = 0$ and that there exists $\mu \in (\frac{1}{4}, 1)$ such that $M_\infty(L_k)^{4\mu} = o\left(M_1(L_k)\right)$ as $k \to +\infty$. Then*

$$\lim_{k\to+\infty} \mathcal{L}(L_k) = \mathcal{L}(\mathcal{C}).$$

More precisely,

$$|\mathcal{L}(\mathcal{C}) - \mathcal{L}(L_k)| = O\Big(\frac{M_\infty(L_k)^{2\mu}}{M_1(L_k)^{1/2}}\Big) + O\big(M_\infty(L_k)^{1-\mu}\big).$$

Proof From the hypothesis, we derive that $\lim_{k\to+\infty} M_\infty(L_k)^{2\mu} = 0$. Then, there exists k_0 such that for any $k > k_0$, $M_\infty(L_k) < 1$. We consider such a $k > k_0$ and we denote by $\left(\zeta_i^k\right)_{i\in\mathbb{Z}/N_k\mathbb{Z}}$, $N_k \in \mathbb{N}$, an ordered sequence of the vertices of the polygon L_k. By definition, L_k splits $\mathcal{C}$ into straightest arcs, so $M_\infty(L_k) < \delta$, for any $i \in \mathbb{Z}/N_k\mathbb{Z}$ the straightest arc $\boldsymbol{C}_i^k$ between ζ_{i-1}^k and ζ_i^k is well defined and $\kappa(\boldsymbol{C}_i^k) \leq \pi/2$.

Let I_0 and I_1 be two subsets of integers defined by:

$$I_0^k := \left\{ i | \kappa(\boldsymbol{C}_i^k) \leq \frac{\pi}{2} M_\infty(L_k)^\mu \right\},$$
$$I_1^k := \mathbb{Z}/N_k\mathbb{Z} \setminus I_0^k.$$

By definition of length and Property 11,

$$\sum_{i=0}^{N_k-1} \|\zeta_{i+1}^k - \zeta_i^k\| \leq \mathcal{L}(\mathcal{C}) \leq \sum_{i=0}^{N_k-1} \frac{\|\zeta_{i+1}^k - \zeta_i^k\|}{\cos\left(\frac{\kappa(\boldsymbol{C}_i^k)}{2}\right)}.$$

Hence,

$$\begin{aligned}
\left|\mathcal{L}(\mathcal{C}) - \sum_{i=0}^{N_k-1} \|\zeta_{i+1}^k - \zeta_i^k\|\right| &\leq \left|\sum_{i=0}^{N_k-1} \frac{\|\zeta_{i+1}^k - \zeta_i^k\|}{\cos\left(\frac{\kappa(\boldsymbol{C}_i^k)}{2}\right)} - \sum_{i=0}^{N_k-1} \|\zeta_{i+1}^k - \zeta_i^k\|\right| \\
&\leq \sum_{i=0}^{N_k-1} \left(\frac{1}{\cos\left(\frac{\kappa(\boldsymbol{C}_i^k)}{2}\right)} - 1\right) \|\zeta_{i+1}^k - \zeta_i^k\|, \\
&\leq \sum_{i\in I_0^k} \left(\frac{1}{\cos\left(\frac{\kappa(\boldsymbol{C}_i^k)}{2}\right)} - 1\right) \|\zeta_{i+1}^k - \zeta_i^k\| \\
&+ \sum_{i\in I_1^k} \left(\frac{1}{\cos\left(\frac{\kappa(\boldsymbol{C}_i^k)}{2}\right)} - 1\right) \|\zeta_{i+1}^k - \zeta_i^k\|.
\end{aligned}$$

On the one hand, since there is at most $\lfloor mM_\infty(L_k)^{-\mu}\rfloor$ arcs $\boldsymbol{C}_i^k$ of turn greater than $M_\infty(L_k)^\mu\pi/2$ in $\mathcal{C}$ where $m := \frac{\kappa(\mathcal{C})}{\pi/2}$ (otherwise, the turn of $\mathcal{C}$ would be greater than $\kappa(\mathcal{C})$), the cardinal of I_1 is such that

$$\# I_1^k \leq mM_\infty(L_k)^{-\mu}.$$

Then,

$$\sum_{i\in I_1}\left(\frac{1}{\cos\left(\frac{\kappa(\boldsymbol{C}_i^k)}{2}\right)}-1\right)\|\zeta_{i+1}^k-\zeta_i^k\| \le \left(\frac{1}{\cos\left(\frac{\pi/2}{2}\right)}-1\right) mM_\infty(L_k)^{1-\mu} \\ = O\left(M_\infty(L_k)^{1-\mu}\right). \tag{5}$$

On the other hand, by Titu's Lemma,

$$\sum_{i\in I_0}\left(\frac{1}{\cos\left(\frac{\kappa(\boldsymbol{C}_i^k)}{2}\right)}-1\right)\|\zeta_{i+1}^k-\zeta_i^k\| \le \\ \sqrt{N_k}\left(\frac{1}{\cos\left(\frac{M_\infty(L_k)^\mu\pi/2}{2}\right)}-1\right)\sqrt{\sum_{i\in I_0}\|\zeta_{i+1}^k-\zeta_i^k\|^2}.$$

Thus, since $M_\infty(L_k)\le 1$, for any $i\in\mathbb{Z}/N_k\mathbb{Z}$, $\|\zeta_{i+1}-\zeta_i\|^2\le\|\zeta_{i+1}-\zeta_i\|$,

$$\sum_{i\in I_0}\left(\frac{1}{\cos\left(\frac{\kappa(\boldsymbol{C}_i^k)}{2}\right)}-1\right)\|\zeta_{i+1}^k-\zeta_i^k\| \le \\ \sqrt{N_k}\left(\frac{1}{\cos\left(\frac{M_\infty(L_k)^\mu\pi/2}{2}\right)}-1\right)\sqrt{\sum_{i\in I_0^k}\|\zeta_{i+1}^k-\zeta_i^k\|}, \\ \le \sqrt{N_k}\left(\frac{1}{\cos\left(\frac{M_\infty(L_k)^\mu\pi/2}{2}\right)}-1\right)\sqrt{\mathcal{L}(L_k)}. \\ \le \sqrt{N_k}\left(\frac{1}{\cos\left(\frac{M_\infty(L_k)^\mu\pi/2}{2}\right)}-1\right)\sqrt{\mathcal{L}(\mathcal{C})}.$$

Moreover,

$$\frac{1}{\cos(y/2)}-1=O(y^2).$$

Hence

$$\sum_{i\in I_0}\left(\frac{1}{\cos\left(\frac{\kappa(\boldsymbol{C}_i^k)}{2}\right)}-1\right)\|\zeta_{i+1}^k-\zeta_i^k\| = O(\sqrt{N_k}M_\infty(L_k)^{2\mu}). \tag{6}$$

Finally, by the equations (5) and (6),

$$\left|\mathcal{L}(\mathcal{C})-\sum_{i=0}^{N_k}\|\zeta_{i+1}^k-\zeta_i^k\|\right| = O(\sqrt{N_k}M_\infty(L_k)^{2\mu})+O(M_\infty(L_k)^{1-\mu}) \\ = O\Big(\frac{M_\infty(L_k)^{2\mu}}{M_1(L_k)^{1/2}}\Big)+O\big(M_\infty(L_k)^{1-\mu}\big)\ . \quad \square$$

In order to use Proposition 3, the parameter μ has to be chosen. Since the speed of convergence is the slowest of $\frac{M_\infty(L_k)^{2\mu}}{M_1(L_k)^{1/2}}$ and $M_\infty(L_k)^{1-\mu}$, the best choice of the parameter is such that

$$M_1(L_k) \sim M_\infty(L_k)^{6\mu-2}.$$

That is, $\mu = 1/2$ for a uniform partition giving an error in $O\left(M_\infty(L_k)^{1/2}\right)$ (in comparison, a polygonal LTB curve randomly sampled provides a linear error). Assuming a Lipschitz continuous turn, the convergence of inscribed polygon lengths toward the true length of the curve can be dramatically speed up: from $M_\infty(L_k)^{1/2}$ to $M_\infty(L_k)^2$ for a uniform sampling. This is the purpose of the next section.

4.1.3 Regular case

In this section, we deal with the case of a LTB-curve whose turn is a Lipschitz function of the arc length, that is the curve is of class $C^{1,1}$, or equivalently, is *par-regular* (for the equivalence between these notions —and also Federer's notion of *reach*— see [19]).

Proposition 4 *Let $\mathcal{C}$ be a δ-LTB curve having a $\frac{1}{r}$-Lipschitz turn. Let (L_k) be a sequence of inscribed polygons splitting the curve $\mathcal{C}$ into straightest arcs such that $\lim_{k\to+\infty} M_\infty(L_k) = 0$. Then*

$$\lim_{k\to+\infty} \mathcal{L}(L_k) = \mathcal{L}(\mathcal{C}).$$

Let $r_1 = \min(r, \delta/2)$ and $(\zeta_i^k)_{i\in\mathbb{Z}/N_k\mathbb{Z}}$ be a cyclically ordered sequence of all the vertices of L_k in $\mathcal{C}$. For any k such that $M_\infty(L_k) < 2r_1$,

$$|\mathcal{L}(\mathcal{C}) - \mathcal{L}(L_k)| \leq \sum_{i=0}^{N_k-1} \left| 2r_1 \arcsin\left(\frac{\|\zeta_i^k - \zeta_{i-1}^k\|}{2r_1}\right) - \|\zeta_i^k - \zeta_{i-1}^k\| \right|.$$

Moreover

$$\sum_{i=0}^{N_k-1} \left| 2r \arcsin\left(\frac{\|\zeta_i^k - \zeta_{i-1}^k\|}{2r}\right) - \|\zeta_i^k - \zeta_{i-1}^k\| \right| = O\left(\frac{(M_3(L_k))^3}{M_1(L_k)}\right).$$

Proof For any k, let $(\zeta_i^k)_{i\in\mathbb{Z}/N_k\mathbb{Z}}$ be a cyclically ordered sequence of the vertices of L_k in $\mathcal{C}$. There exists k_0, such that for any $k > k_0$, $M_\infty(L_k) < 2r_1$. By [19, Lemma 2.11], for any $i \in \mathbb{Z}/N_k\mathbb{Z}$, the straightest arc $\boldsymbol{C}_{\zeta_{i-1}^k,\zeta_i^k}$ between ζ_{i-1}^k and ζ_i^k is such that

$$\mathcal{L}(\boldsymbol{C}_{\zeta_{i-1}^k,\zeta_i^k}) \leq 2r_1 \arcsin\left(\frac{\|\zeta_i^k - \zeta_{i-1}^k\|}{2r_1}\right).$$

Since the function $x \mapsto 2r_1 \arcsin(\frac{x}{2r_1}) - x$ is increasing on $[0, 2r_1)$, for any k such that $M_\infty(L_k) < 2r_1$,

$$\begin{aligned} |\mathcal{L}(\mathcal{C}) - \mathcal{L}(L_k)| &\leq \sum_{i=0}^{N_k-1} \left| 2r_1 \arcsin\left(\frac{\|\zeta_i^k - \zeta_{i-1}^k\|}{2r_1}\right) - \|\zeta_i^k - \zeta_{i-1}^k\| \right|, \\ &\leq N_k \left(2r_1 \arcsin\left(\frac{M_\infty(L_k)}{2r_1}\right) - M_\infty(L_k) \right). \end{aligned}$$

Moreover,

$$\arcsin(x) = x + O(x^3) \quad \text{as } x \to 0.$$

Then,

$$\begin{aligned}
|\mathcal{L}(\mathcal{C}) - \mathcal{L}(L_k)| &\leq \sum_{i=0}^{N_k-1} \left| 2r_1 \arcsin\left(\frac{\|\zeta_i^k - \zeta_{i-1}^k\|}{2r_1}\right) - \|\zeta_i^k - \zeta_{i-1}^k\| \right|, \\
&\leq N_k \; O\left((M_3(L_k))^3\right) \\
&\leq \frac{\mathcal{L}(\mathcal{C})}{M_1(L_k)} \; O\left((M_3(L_k))^3\right), \\
&\leq O\left(\frac{(M_3(L_k))^3}{M_1(L_k)}\right) \quad . \quad \square
\end{aligned}$$

The bound of Proposition 4 is sharp. Indeed, for a circle of radius r and a uniform and tight enough partition of the circle, one has:

$$\begin{aligned}
|\mathcal{L}(\mathcal{C}) - \mathcal{L}(L_k)| &= \sum_{i=0}^{N_k-1} \left| 2r \arcsin\left(\frac{\|\zeta_i^k - \zeta_{i-1}^k\|}{2r}\right) - \|\zeta_i^k - \zeta_{i-1}^k\| \right|, \\
&= N_k \left(2r \arcsin\left(\frac{M_\infty(L_k)}{2r}\right) - M_\infty(L_k) \right) \\
&= O\left(\frac{(M_3(L_k))^3}{M_1(L_k)}\right).
\end{aligned}$$

Proposition 4 can be compared to [21, Proposition 3]. We get the same rate of convergence replacing the convexity hypothesis by the local turn boundedness hypothesis.

To complete the determination of the convergence speed of polygon lengths toward the length of a LTB curve, it is necessary to study the weight of the error due to the use of discrete chords instead of Euclidean chords. This is the goal of the next section.

4.2 LTB curve length estimation by means of polygons inscribed in the curve digitization

Given a LTB curve $\mathcal{C}$ and the family of its Gauss digitizations $\{\mathrm{Dig}_h(\mathcal{C})\}_{h>0}$, the results obtained in Sections 3 and 4.1 make it possible to build a convergent estimator of the curve length $\mathcal{L}(\mathcal{C})$ using polygons $\mathcal{A}_h$ inscribed in the reconstructions $\partial_h(\mathcal{C})$ under some assumptions on their edge lengths. At a fixed resolution, the estimated length is the length $\mathcal{L}(\mathcal{A}_h)$. The two following theorems specify these assumptions, and give the convergence rate, in the general case then in the regular case.

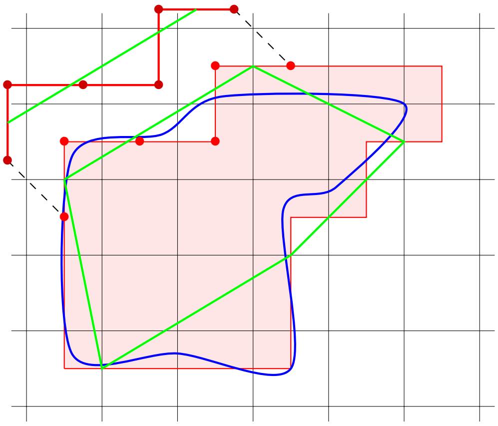

Figure 17: In blue, a LTB curve $\mathcal{C}$. The reconstruction of $\mathcal{C}$ (red border) is partitionned into subarcs (as the one emphasized in the figure). To each subarc corresponds an edge whose ends are on the ending bels of the subarc. The union of all these edges forms a polygon $\mathcal{A}_h$ (green) inscribed in $\partial_h(C)$. The length of the curve $\mathcal{C}$ is estimated by the length of $\mathcal{A}_h$.

4.2.1 General case

The length estimator used in the article is based on the choice of a few bels of $\mathrm{Bel}_h(\mathcal{C})$. The midpoints of these bels are the vertices of a polygon A_h whose length estimates the length of the curve $\mathcal{C}$ (see Figure 17). The rate of convergence of the estimation error towards 0 is a trade off between two parts of the error. The first part which is $O_{h\to 0}(M_\infty(\mathcal{A}_h)^{2\mu} M_1(\mathcal{A}_h)^{-1/2} + M_\infty(\mathcal{A}_h)^{1-\mu})$ in the general case, corresponds to the difference between the length of the curve and the length of the polygon $\xi(\mathcal{A}_h)$ inscribed in it (calculated in Proposition 3). It converges toward 0 because of the hypothesis $\lim_{h\to 0} M_1(\mathcal{A}_h) = 0$. The condition $M_\infty(\mathcal{A}_h)^{4\mu} = o(M_1(\mathcal{A}_h))$, also inherited from Proposition 3, is explained just before it. The second part, $hN_h = O_{h\to 0}\frac{h}{M_1(\mathcal{A}_h)}$ corresponds to the difference in length of the polygon $\mathcal{A}_h$ inscribed in $\partial_h(\mathcal{C})$ and of the back-digitized polygon $\xi(\mathcal{A}_h)$ inscribed in $\mathcal{C}$, where N_h stands for the number of sides of $\mathcal{A}_h$. The second part converges toward 0 if the mean length $M_1(\mathcal{A}_h)$ converges toward 0 slower than the grid step h. The remaining hypothesis (each vertex of $\mathcal{A}_h$ lies on a bel of the normal subsequence) ensures that the vertices of $\mathcal{A}_h$ are back-digitized on $\mathcal{C}$ in the order defined on it.

Theorem 2 *Let $\mathcal{C}$ be a δ-LTB curve with $\delta > 0$. Let $\mu \in (\frac{1}{4}, 1)$ and $\{\mathcal{A}_h\}_{h>0}$ be a family of polygons such that*

- *for any h compatible with $\mathcal{C}$, the vertices of $\mathcal{A}_h$ are the bel middles of a normal subsequence of the cyclically ordered bels $(b_i^h)_{i\in\mathbb{Z}/N\mathbb{Z}}$,*
- *$h = o(M_1(\mathcal{A}_h))$ as $h \to 0$,*
- *$M_\infty(\mathcal{A}_h)^{4\mu} = o\left(M_1(\mathcal{A}_h)\right) = o(1)$ as $h \to 0$.*

Then,

$$\lim_{h\to 0} \mathcal{L}(\mathcal{A}_h) = \mathcal{L}(\mathcal{C}).$$

More precisely,

$$\|\mathcal{L}(\mathcal{C}) - \mathcal{L}(\mathcal{A}_h)\| = O_{h\to 0}\left(M_\infty(\mathcal{A}_h)^{2\mu} M_1(\mathcal{A}_h)^{-1/2} + M_\infty(\mathcal{A}_h)^{1-\mu} + hM_1(\mathcal{A}_h)^{-1}\right).$$

Proof Let $\xi : \mathrm{Bel}_h(\mathcal{C}) \to \mathcal{C}$ be a back-digitization and $(b_i^h)_{i\in\mathbb{Z}/N_h\mathbb{Z}}$ be a normal subsequence of $\mathrm{Bel}_h(\mathcal{C})$ defining the polygon $\mathcal{A}_h$. Write m_i^h for the middle of b_i^h and let L_h be the polygon whose ordered set of vertices is $\xi((b_i^h)_{i\in\mathbb{Z}/N_h\mathbb{Z}})$. Then,

$$|\mathcal{L}(\mathcal{C}) - \mathcal{L}(\mathcal{A}_h)| \leq |\mathcal{L}(\mathcal{C}) - \mathcal{L}(L_h)| + |\mathcal{L}(L_h) - \mathcal{L}(\mathcal{A}_h)|.$$

By definition of a back-digitization, $\mathrm{d}(m_i^h, \xi(b_i^h)) < h/2$ for any i, so $|\mathcal{L}(L_h) - \mathcal{L}(\mathcal{A}_h)|$ is bounded from above by $N_h \times h$, that is by $h/M_1(\mathcal{A}_h) \times \mathcal{L}(\mathcal{A}_h)$. Since $\mathcal{L}(L_h) < \mathcal{L}(\mathcal{C})$ and we assume $\lim_{h\to 0} h/M_1(\mathcal{A}_h) = 0$, using the triangle inequality, we can bound from above $\mathcal{L}(A_h)$ by some constant (for instance $2\mathcal{L}(\mathcal{C})$ for $h/M_1(\mathcal{A}_h) \leq 1/2$). We derive that

$$|\mathcal{L}(L_h) - \mathcal{L}(\mathcal{A}_h)| = O_{h\to 0}\left(\frac{h}{M_1(\mathcal{A}_h)}\right).$$

By Theorem 1, (b_i^h) delimits straightest arcs of $\mathcal{C}$. Hence, thanks to Proposition 3, we get

$$|\mathcal{L}(\mathcal{C}) - \mathcal{L}(\mathcal{A}_h)| = O_{h\to 0}\left(\frac{M_\infty(L_h)^{2\mu}}{M_1(L_h)^{1/2}} + M_\infty(L_h)^{1-\mu} + \frac{h}{M_1(\mathcal{A}_h)}\right).$$

Moreover, $M_\infty(L_h) \leq M_\infty(\mathcal{A}_h) + h$. Then,

$$|\mathcal{L}(\mathcal{C}) - \mathcal{L}(\mathcal{A}_h)| = O_{h\to 0}\left(\frac{(M_\infty(\mathcal{A}_h) + h)^{2\mu}}{M_1(\mathcal{A}_h)^{1/2}} + (M_\infty(\mathcal{A}_h) + h)^{1-\mu} + \frac{h}{M_1(\mathcal{A}_h)}\right).$$

Finally, since h is dominated asymptotically by $M_1(\mathcal{A}_h)$ which is less than $M_\infty(\mathcal{A}_h)$,

$$|\mathcal{L}(\mathcal{C}) - \mathcal{L}(\mathcal{A}_h)| = O_{h\to 0}\left(\frac{M_\infty(\mathcal{A}_h)^{2\mu}}{M_1(\mathcal{A}_h)^{1/2}} + M_\infty(\mathcal{A}_h)^{1-\mu} + \frac{h}{M_1(\mathcal{A}_h)}\right). \quad \square$$

Theorem 2 gives indication in order to choose the best sampling of the curve. For a fixed $M_\infty(\mathcal{A}_h)$, the best rate of convergence for an unknown curve $\mathcal{C}$ is reached when $M_1(\mathcal{A}_h)$ is maximum, that is when $M_1(\mathcal{A}_h) = M_\infty(\mathcal{A}_h)$: the inscribed polygons associated with the family $\{\mathcal{A}_h\}$ have equal edges. In this latter case the rate of convergence is $O\big(M_\infty(\mathcal{A}_h)^{1/2} + hM_\infty(\mathcal{A}_h)^{-1}\big)$ (by choosing $\mu = \frac{1}{2} = \max_{\mu\in(0,1)} \min(2\mu - 1/2, 1 - \mu)$). Since $h^{2/3} = \operatorname{argmin}_{x>0} \max(\sqrt{x}, h/x)$, the best rate of convergence, $h^{1/3}$, is achieved for $M_\infty(\mathcal{A}_h) \sim h^{2/3}$.

4.2.2 Regular case

Theorem 3 *Let $\mathcal{C}$ be a δ-LTB curve having a $\frac{1}{r}$-Lipschitz turn ($r > 0$). Let $\{\mathcal{A}_h\}_{h>0}$ be a family of polygons such that*

- *for any h compatible with $\mathcal{C}$,the vertices of $\mathcal{A}_h$ are the bel middles of a normal subsequence of the cyclically ordered bels $(b_i)_{i\in\mathbb{Z}/N\mathbb{Z}}$,*
- *$h = o_{h\to 0}(M_1(\mathcal{A}_h))$,*
- *$\lim_{h\to 0} M_\infty(\mathcal{A}_h) = 0$.*

Then,

$$\lim_{h\to 0} \mathcal{L}(\mathcal{A}_h) = \mathcal{L}(\mathcal{C})$$

and,

$$|\mathcal{L}(\mathcal{C}) - \mathcal{L}(\mathcal{A}_h)| = O_{h\to 0}\left(\frac{M_3(\mathcal{A}_h)^3}{M_1(\mathcal{A}_h)}\right).$$

Moreover, for any h compatible with $\mathcal{C}$ such that $h + M_\infty(\mathcal{A}_h) < 2r_1$ with $r_1 = \min(r, \delta/2)$, we have

$$|\mathcal{L}(\mathcal{C}) - \mathcal{L}(\mathcal{A}_h)| \leq N_h\left(2r_1 \arcsin\left(\frac{M_\infty(\mathcal{A}_h) + h}{2r_1}\right) - M_\infty(\mathcal{A}_h)\right),$$

Proof Let h be compatible with $\mathcal{C}$ and $\xi : \mathrm{Bel}_h(\mathcal{C}) \to \mathcal{C}$ be a back-digitization. As in the proof of Theorem 2, we have

$$|\mathcal{L}(\mathcal{C}) - \mathcal{L}(\mathcal{A}_h)| \leq |\mathcal{L}(\mathcal{C}) - \mathcal{L}(L_h)| + hN_h,$$

where L_h is the polygon whose vertices are the images by ξ of the bels defining $\mathcal{A}_h$. By Theorem 1, the vertices of L_h delimit straightest arcs of $\mathcal{C}$. Let $(\zeta_i^h)_{i\in\mathbb{Z}/N_k\mathbb{Z}}$ be a cyclically ordered sequence of vertices of L_h in $\mathcal{C}$. Assuming $h + M_\infty(\mathcal{A}_h) < 2r_1$, we derive from Proposition 4 that,

$$|\mathcal{L}(\mathcal{C}) - \mathcal{L}(L_k)| \leq \sum_{i=0}^{N_h-1} \left|2r_1 \arcsin\left(\frac{\|\zeta_i^h - \zeta_{i-1}^h\|}{2r_1}\right) - \|\zeta_i^h - \zeta_{i-1}^h\|\right| \tag{7}$$

Since the function $x \mapsto 2r_1 \arcsin\left(\frac{x}{2r_1}\right) - x$ is non-negative and increasing on $[0, 2r_1)$,

$$\begin{aligned}
|\mathcal{L}(\mathcal{C}) - \mathcal{L}(\mathcal{A}_h)| &\leq \sum_{i=0}^{N_h-1} \left(2r_1 \arcsin\left(\frac{\|\zeta_i^h - \zeta_{i-1}^h\| + h}{2r_1}\right) - \|\zeta_i^h - \zeta_{i-1}^h\| - h\right) \\
&\quad + hN_h \\
&\leq \sum_{i=0}^{N_h-1} \left(2r_1 \arcsin\left(\frac{\|\zeta_i^h - \zeta_{i-1}^h\| + h}{2r_1}\right) - \|\zeta_i^h - \zeta_{i-1}^h\|\right) \\
&\leq N_h\left(2r_1 \arcsin\left(\frac{M_\infty(\mathcal{A}_h) + h}{2r_1}\right) - M_\infty(\mathcal{A}_h)\right).
\end{aligned}$$

Moreover,

$$\arcsin(x) = x + O(x^3) \quad \text{as } x \to 0.$$

Then, from Equation 7, we derive

$$\begin{aligned}
|\mathcal{L}(\mathcal{C}) - \mathcal{L}(\mathcal{A}_h)| &\leq \sum_{i=0}^{N_h-1} \left(2r_1 \arcsin\left(\frac{\|\zeta_i^h - \zeta_{i-1}^h\|}{2r_1} \right) - \|\zeta_i^h - \zeta_{i-1}^h\| \right) + hN_h, \\
&\leq N_h \left(O\left(M_3(\mathcal{A}_h)^3 \right) + h \right) \\
&\leq \frac{\mathcal{L}(\mathcal{C})}{M_1^h(\mathcal{A}_h)} O\left(M_3(\mathcal{A}_h)^3 + h \right), \\
&\leq O\left(\frac{M_3(\mathcal{A}_h)^3 + h}{M_1^h} \right).
\end{aligned}$$

Since $h = o(M_1(\mathcal{A}_h))$ and $M_1(\mathcal{A}_h) \leq M_3(\mathcal{A}_h)$, we obtain the result:

$$|\mathcal{L}(\mathcal{C}) - \mathcal{L}(\mathcal{A}_h)| = O\left(\frac{M_3^3(\mathcal{A}_h)}{M_1^h} \right) \quad . \quad \square$$

Observe that, by [18, Theorem 2], any par(r)-regular curve $\mathcal{C}$ is $\sqrt{2}r$-LTB and by [18, Lemma 6], its turn is $\frac{1}{r}$ Lipschitz. Thus, Theorem 3 applies to par(r)-regular curves taking $r_1 = \min(r, \delta/2) = \min(r, r/\sqrt{2}) = r/\sqrt{2}$.

Application of theorems 2 and 3 on classical estimators requires some more work and will be detailed in future works.

5 Conclusion

The starting point of the study presented in this paper is the couple of articles [21, 20] about convergence of length estimators. The main idea in these articles, originally stated in [29], is that —a contrary to length estimation in a pure Euclidean context— estimating a length from a digital sample cannot be performed by just picking more and more points on the boundary of the digitization. The picking has to be sparse relative to the grid step. In the cited articles, the result was established for graphs of functions and we thought at the time that it could be straightforwardly adapted on Jordan curves. The content of this paper shows that it is far to be the case. It is easy to project the OBQ digitization of a graph of function on this graph even for non-regular curves. Getting a well-ordered sample on a Jordan curve from its digitization is another challenge as shown in Figure 12. A first step in this direction was done in [13]. Nevertheless, it assumes $C^{1,1}$ regularity and, though the size of the defective regions is quantified, the well-ordering is not guaranteed. This has led us to introduce the notion of LTB curve in [18]. The LTB class encompasses the $C^{1,1}$ curves since we show that $C^{1,1}$ regularity is equivalent to be LTB with a Lipschitz turn. Then we formally establish in this paper that the LTB class of curves is sufficiently constrained to permit ordered projections (though the class contains non-regular curves). Once a reliable kind of projection —the monotonic sampler— is found, proving the multigrid convergence of non-local perimeter estimators does not give rise to great difficulties.

Furthermore, our results about length estimation may also be applied to arcs of a LTB curve. Indeed, on the one hand, same calculations as those on the whole Jordan curve (Theorem 2 or Theorem 3) can be carried out for curve arcs. On the other hand, the back-digitization defined on the Jordan curve (Theorem 1) should permit to put in correspondence a sparse (but tight enough) partition of a digital arc to a partition in straightest arcs of the underlying continuous curve. Nevertheless, it supposes to rewrite all the propositions.

Nevertheless, it remains to study in a future work whether the error bounds exhibited in this article are tight or not. Indeed, for a particular Jordan curve, the worst case considered in the upper bound calculus is only reached at a given resolution. Then, it may be possible to improve the error upper bound. In the perimeter estimation, the convexity hypothesis is often used to obtain upper bounds, e.g. for Non-Local estimation, the convexity hypothesis makes it possible to approach experimental convergence speed. As the turn can be seen as a measure of the convexity loss, it can be interesting to see if the results obtained in the convex case in the literature can be generalized to LTB curves.

Another direction to continue the work done in this paper is to use the back-digitization to prove the multigrid convergence of the MDSS based perimeter estimators on LTB curves.

The back-digitization could also be used for the estimation of other geometric features. In particular, since the definition of the back-digitization relies on the notion of turn, it should be well-suited for curvature estimation. A last perspective concerns the generalization of the LTB notion to 3D curves and surfaces.

References

1. Alexandrov, A.D., Reshetnyak, Y.G.: General Theory of Irregular Curves. Kluwer Academic Pulishers (1989)
2. Asano, T., Kawamura, Y., Klette, R., Obokata, K.: Minimum-length polygons in approximation sausages. In: C. Arcelli, L.P. Cordella, G.S. Baja (eds.) Visual Form 2001, *Lecture Notes in Computer Science*, vol. 2059, pp. 103–112. Springer Berlin Heidelberg (2001). DOI 10.1007/3-540-45129-3_8
3. Chazal, F., Cohen-Steiner, D., Lieutier, A.: A sampling theory for compact sets in Euclidean space. Discrete & Computational Geometry **41**(3), 461–479 (2009). DOI 10.1007/s00454-009-9144-8. URL https://doi.org/10.1007/s00454-009-9144-8
4. Cœurjolly, D., Klette, R.: A comparative evaluation of length estimators of digital curves. IEEE Trans. Pattern Anal. Mach. Intell. **26**(2), 252–257 (2004)
5. Coeurjolly, D., Lachaud, J.O., Levallois, J.: Integral based curvature estimators in digital geometry. In: B.M. R. Gonzalez-Diaz M.J. Jimenez (ed.) 17th International Conference on Discrete Geometry for Computer Imagery (DGCI 2013), Lecture Notes in Computer Science, pp. 215–227. Springer Verlag (2013). URL http://liris.cnrs.fr/publis/?id=5866
6. Coeurjolly, D., Lachaud, J.O., Roussillon, T.: Multigrid convergence of discrete geometric estimators. In: V. Brimkov, R. Barneva (eds.) Digital Geometry Algorithms, Theoretical Foundations and Applications of Computational Imaging, *Lecture Notes in Computational Vision and Biomechanics*, vol. 2, pp. 395–424. Springer-Verlag (2012)
7. Daurat, A., Tajine, M., Zouaoui, M.: Les estimateurs semi-locaux de périmètre. Tech. rep. (2011). URL https://hal.archives-ouvertes.fr/hal-00576881
8. Federer, H.: Curvature measures. Transactions of the American Mathematical Society **93**(3), 418–491 (1959). URL http://www.jstor.org/stable/1993504
9. Klette, R., Rosenfeld, A.: Geometric Methods for Digital Picture Analysis. Elsevier (2004)
10. Klette, R., Žunić, J.: Multigrid convergence of calculated features in image analysis. Journal of Mathematical Imaging and Vision **13**(3), 173–191 (2000)
11. Klette, R., Yang, N.: Measurements of arc length's by shortest polygonal jordan curves. http://citr.auckland.ac.nz/techreports/1998/CITR-TR-26.pdf (1998)
12. Klette, R., Yip, B.: Evaluation of curve length measurements. Proc 1st Int Conf on Pattern Recognition **1**, 1610 (2000)

13. Lachaud, J., Thibert, B.: Properties of gauss digitized shapes and digital surface integration. J. Math. Imaging Vis. **54**(2), 162–180 (2016). DOI 10.1007/s10851-015-0595-7. URL https://doi.org/10.1007/s10851-015-0595-7
14. Lachaud, J.O.: Espaces non-euclidiens et analyse d'image : modèles déformables riemanniens et discrets, topologie et géométrie discrète. Habilitation à diriger des recherches en informatique, Université Sciences et Technologies, Bordeaux I (2006)
15. Latecki, L., Eckhardt, U., Rosenfeld, A.: Well-composed sets. Computer Vision and Image Understanding **61**(1), 70–83 (1995). DOI http://dx.doi.org/10.1006/cviu.1995.1006
16. Latecki, L.J., Conrad, C., Gross, A.: Preserving topology by a digitization process. Journal of Mathematical Imaging and Vision **8**, 131–159 (1998)
17. Le Quentrec, É., Mazo, L., Baudrier, É., Tajine, M.: Local turn-boundedness: A curvature control for a good digitization. In: M. Couprie, J. Cousty, Y. Kenmochi, N. Mustafa (eds.) Discrete Geometry for Computer Imagery, pp. 51–61. Springer International Publishing, Cham (2019)
18. Le Quentrec, E., Mazo, L., Baudrier, E., Tajine, M.: Local turn-boundedness, a curvature control for continuous curves with application to digitization. Journal of Mathematical Imaging and Vision **62**, 673–692 (2020). DOI https://doi.org/10.1007/s10851-020-00952-x. URL http://icube-publis.unistra.fr/2-LMBT20
19. Le Quentrec, E., Mazo, L., Baudrier, É., Tajine, M.: LTB curves with Lipschitz turn are par-regular. Research Report, Laboratoire ICube, université de Strasbourg (2021). URL https://hal.archives-ouvertes.fr/hal-03480735v1
20. Mazo, L., Baudrier, É.: Non-local estimators: a new class of multigrid convergent length estimators. Theoretical Computer Science **645**, 128–146 (2016). DOI 10.1016/j.tcs.2016.07.007. URL http://icube-publis.unistra.fr/2-MB16
21. Mazo, L., Baudrier, E.: Non-local length estimators and concave functions. Theoretical Computer Science **690**, 73–90 (2017). DOI 10.1016/j.tcs.2017.06.005. URL http://icube-publis.unistra.fr/2-MB17
22. Meine, H., Köthe, U., Stelldinger, P.: A topological sampling theorem for robust boundary reconstruction and image segmentation. Discrete Applied Mathematics **157**(3), 524–541 (2009). DOI https://doi.org/10.1016/j.dam.2008.05.031. URL http://www.sciencedirect.com/science/article/pii/S0166218X08002643. International Conference on Discrete Geometry for Computer Imagery
23. Milnor, J.W.: On the total curvature of knots. Annals of Mathematics, Second Series **52**, 248–257 (1950)
24. Ngo, P., Passat, N., Kenmochi, Y., Debled-Rennesson, I.: Geometric preservation of 2D digital objects under rigid motions. Journal of Mathematical Imaging and Vision **61**, 204–223 (2019). DOI 10.1007/s10851-018-0842-9. URL https://hal.univ-reims.fr/hal-01695370
25. Pavlidis, T.: Algorithms for graphics and image processing. Springer-Verlag Berlin-Heidelberg (1982)
26. Serra, J.: Image Analysis and Mathematical Morphology. Academic Press, Inc., USA (1983)
27. Sloboda, F., Zatko, B., Stoer, J.: On approximation of planar one-dimensional continua. Advances in Digital and Computational Geometry pp. 113–160 (1998)
28. Stelldinger, P., Terzic, K.: Digitization of non-regular shapes in arbitrary dimensions. Image and Vision Computing **26**(10), 1338–1346 (2008). DOI https://doi.org/10.1016/j.imavis.2007.07.013. URL http://www.sciencedirect.com/science/article/pii/S0262885607001370
29. Tajine, M., Daurat, A.: Patterns for multigrid equidistributed functions: Application to general parabolas and length estimation. Theoretical Computer Science **412**(36), 4824 – 4840 (2011)
30. de Vieilleville, F., Lachaud, J.O.: Experimental comparison of continuous and discrete tangent estimators along digital curves. In: V.E. Brimkov, R.P. Barneva, H.A. Hauptman (eds.) Combinatorial Image Analysis, pp. 26–37. Springer Berlin Heidelberg, Berlin, Heidelberg (2008)
31. de Vieilleville, F., Lachaud, J.O., Feschet, F.: Maximal digital straight segments and convergence of discrete geometric estimators. In: H. Kalviainen, J. Parkkinen, A. Kaarna (eds.) Image Analysis, pp. 988–997. Springer Berlin Heidelberg, Berlin, Heidelberg (2005)
32. de Vieilleville, F., Lachaud, J.O., Feschet, F.: Maximal digital straight segments and convergence of discrete geometric estimators. Journal of Mathematical Image and Vision **27**(2), 471–502 (2007)